arXiv:1701.07714v2 [math.AG] 2 Feb 2017

Discriminant circle bundles over local models of Strebel graphs and Boutroux curves

M.Bertola and D.Korotkin

February 3, 2017

Abstract

We study special "discriminant" circle bundles over two elementary moduli spaces of meromorphic quadratic differentials with real periods denoted by $\mathcal{Q}_0^{\mathbb{R}}(-7)$ and $\mathcal{Q}_0^{\mathbb{R}}([-3]^2)$. The space $\mathcal{Q}_0^{\mathbb{R}}(-7)$ is the moduli space of meromorphic quadratic differentials on the Riemann sphere with one pole of order 7 with real periods; it appears naturally in the study of a neighbourhood of the Witten's cycle W_1 in the combinatorial model based on Jenkins-Strebel quadratic differentials of $\mathcal{M}_{g,n}$. The space $\mathcal{Q}_0^{\mathbb{R}}([-3]^2)$ is the moduli space of meromorphic quadratic differentials on the Riemann sphere with two poles of order at most 3 with real periods; it appears in description of a neighbourhood of Kontsevich's boundary $W_{-1,-1}$ of the combinatorial model. The application of the formalism of the Bergman tau-function to the combinatorial model (with the goal of computing analytically Poincare dual cycles to certain combinations of tautological classes) requires the study of special sections of circle bundles over $\mathcal{Q}_0^{\mathbb{R}}(-7)$ and $\mathcal{Q}_0^{\mathbb{R}}([-3]^2)$; in the case of the space $\mathcal{Q}_0^{\mathbb{R}}(-7)$ a section of this circle bundle is given by the argument of the modular discriminant. We study the spaces $\mathcal{Q}_0^{\mathbb{R}}(-7)$ and $\mathcal{Q}_0^{\mathbb{R}}([-3]^2)$, also called the spaces of Boutroux curves in detail, together with corresponding circle bundles.

Contents

1 Motivation and summary of results **2**

2 Combinatorial model of $\mathcal{M}_{g,n}$ via Jenkins-Strebel differentials **4**

3 A local model near Witten's cycle W_1: the space $Q_0^{\mathbb{R}}(-7)$ **7**
3.1 Resolution of a 5-valent vertex by flat surgery 7
3.2 Plumbing construction 10

4 A local model near Kontsevich's boundary $W_{-1,-1}$ and space $Q_0^{\mathbb{R}}([-3]^2)$ **11**
4.1 Resolution of two one-valent vertices by flat surgery 12
4.2 Plumbing construction 14

5 Modular discriminant Δ_1 on the space $\mathcal{Q}_0^{\mathbb{R}}(-7)$ **14**
5.1 Space $\mathcal{Q}_0(-7)$ 14
5.2 Real slice $\mathcal{Q}_0^{\mathbb{R}}(-7)$: Boutroux curves 16
5.3 Variation of $\arg\Delta_1$ on $\mathcal{Q}_0^{\mathbb{R}}(-7)$ 23

6 Arguments of $\Delta^{\pm}_{-1,-1}$ on the space $\mathcal{Q}_0^{\mathbb{R}}([-3]^2)$ **25**
6.1 Space $Q_0([-3]^2)$ 25
6.2 Real slice $Q_0^{\mathbb{R}}([-3]^2)$: Boutroux curves 26
6.3 Variation of $\arg\Delta^{\pm}_{-1,-1}$ on $\mathcal{Q}_0^{\mathbb{R}}([-3]^2)$ 27

A Proof of Proposition 2 **29**

1 Motivation and summary of results

The combinatorial model $\mathcal{M}_{g,n}^{comb}$ of the moduli spaces $\mathcal{M}_{g,n}$ (for $n \geq 1$) based on Jenkins-Strebel differentials [11, 25, 7, 8] was proven to be very fruitful in studies of geometry of the moduli space. In particular, it was used in Kontsevich's proof [12, 13] of Witten's conjecture [26] about intersection numbers of ψ-classes.

In this approach the combinatorial model is a CW complex in which each cell is homeomorphic to a simplex labelled by fatgraphs embedded on a Riemann surface. It was shown in [9, 10, 22, 23], following earlier work [24] (where the combinatorial model of $\mathcal{M}_{g,n}$ based on hyperbolic geometry was used) and [1] that natural cycles in the combinatorial model can be interpreted as Poincaré duals to certain combinations of Miller-Morita-Mumford classes, or kappa-classes. These natural cycles consist of cells corresponding to fatgraphs with fixed odd valencies of vertices: cells of highest dimension correspond to three-valent fatgraphs. If the fatgraph contains only one vertex of valency different from 3 then such cycles are called "Witten's cycles"; if the number of such non-generic vertices is bigger than one, the corresponding union of cells is called "Kontsevich cycle". A particular role is played by the following two cycles; the first cycle is the Witten's cycle W_1 which contains fatgraphs with one vertex of valency 5 and other vertices of valency 3. The second cycle is the Kontsevich's boundary $W_{-1,-1}$ of the combinatorial model, containing fatgraphs which have two vertices of valency 1 and all other vertices of valency 3. The Kontsevich's boundary $W_{-1,-1}$ is a subset of Deligne-Mumford boundary of $\mathcal{M}_{g,n}$ (some components of the DM boundary are mapped to a point in $W_{-1,-1}$).

In general, the Kontsevich–Witten cycle $W_{(k_1,\dots,k_r)}$ consists of cells corresponding to Strebel graphs where r vertices have valency $2k_j+3$ respectively ($k_j \geq -1$) and all the others have valency 3 (see [9]).

The starting point of computations relating combinatorial cycles to κ-classes and their combinations is the explicit expression for the connection forms in circle bundles (or $U(1)$ bundles) which correspond to tautological line bundles $\mathcal{L}_k$ associated to the k–th puncture, see [12, 28] and [9, 22, 23] for details.

The main motivation of this work is to provide the analytical background for an application of the techniques of the Bergman tau-function to the combinatorial model $\mathcal{M}_{g,n}^{comb}$ of $\mathcal{M}_{g,n}$. The Bergman tau-function first appeared in the theory of isomonodromic deformations [17] and Frobenius manifolds [5] in the context on Hurwitz spaces. It was then extended to the moduli spaces of Abelian [14] and quadratic differentials [15] over Riemann surfaces. Geometrically, the Bergman tau-function is a (holomorphic or meromorphic) section of the product of Hodge line bundle and other natural line bundles over the corresponding moduli space. Therefore, in a holomorphic framework, an analysis of its singularity structure allows to derive various relations in the Picard groups of these moduli spaces [20, 18, 19]. The direct application of this technique in the context of combinatorial model of $\mathcal{M}_{g,n}$ based on JS differentials is problematic due to the absence of a natural holomorphic structure of the cells. The Bergman tau-function appropriately defined on the Jenkins-Strebel combinatorial model of $\mathcal{M}_{g,n}$ is only real-analytic in each cell; however, its argument can still be used to get a smooth section of a circle bundle. In turn, study of monodromy of these sections allows us to find cycles of the combinatorial model which are Poincaré dual to certain combinations of standard tautological classes on $\mathcal{M}_{g,n}$ [3]. The implementation of this idea requires the study of the local behaviour of the Bergman tau-function and corresponding circle bundle in a neighbourhood of the cycles W_1 and $W_{-1,-1}$.

Hereafter we describe neighbourhoods of W_1 and $W_{-1,-1}$ in $\mathcal{M}_{g,n}^{comb}$ by applying an appropriate "flat welding" which equivalently can be interpreted via the "plumbing" construction using the flat structure introduced on a Riemann surface by the JS differential.

Combinatorial model near W_1 and $W_{-1,-1}$. The study of a neighbourhood of the Witten's cycle W_1 in $\mathcal{M}_{g,n}^{comb}$ leads to the appearance of the real slice $\mathcal{Q}_0^{\mathbb{R}}(-7)$ (space of "Boutroux curves") of the moduli space, $\mathcal{Q}_0(-7)$, of meromorphic quadratic differentials on Riemann sphere with one pole of order 7.

The space $\mathcal{Q}_0^{\mathbb{R}}(-7)$ appears in the study of a neighbourhood of $W_1 \subset \mathcal{M}_{g,n}^{comb}$ as follows; cells forming the cycle W_1 are obtained from cells of highest dimension of $\mathcal{M}_{g,n}^{comb}$ by contraction of two edges having exactly one common vertex; this contraction gives rise to the creation of a "plumbing zone" as shown in Fig. 6 which separates a component $\mathbb{CP}^1$ containing the three zeros of Q and a pole of Q of degree 7 at the nodal point. Thus the quadratic differential Q arising on the separated Riemann sphere belongs to the space $Q_0^{\mathbb{R}}(-7)$.

The space $\mathcal{Q}_0^{\mathbb{R}}([-3]^2)$ appears in a neighbourhood of Kontsevich's boundary $W_{-1,-1}$: it is the moduli space of quadratic differentials on the Riemann sphere with two poles of order 3. The cells forming $W_{-1,-1}$ are obtained

from the cells of the highest dimension by simultaneous contraction of two edges having two common vertices. Such a contraction creates two "plumbing zones" as shown in Fig. 10; the Riemann sphere arising between the plumbing zones contains two simple zeros of Q and two poles of degree 3 at the arising nodal points. Thus the quadratic differential Q arising on the separating Riemann sphere is an element of the space $Q_0^{\mathbb{R}}([-3]^2,[1]^2)$.

Both spaces $\mathcal{Q}_0^{\mathbb{R}}(-7)$ and $\mathcal{Q}_0^{\mathbb{R}}([-3]^2)$ have real dimension 2. Surprisingly enough, we did not find a complete self-contained description of these two elementary moduli spaces in the literature; one of the goals of the paper is to fill this gap.

The stratification of these spaces as well as their complexified versions $\mathcal{Q}_0(-7)$ and $\mathcal{Q}_0([-3]^2)$, respectively, is studied in detail in Sections 5.1, 6.1.

Space $\mathcal{Q}_0^{\mathbb{R}}(-7)$. The generic element of the complex space $\mathcal{Q}_0(-7)$ can be represented by the quadratic differential

$$Q=(x-x_1)(x-x_2)(x-x_3)(\mathrm{d}x)^2\ ,\quad x_1+x_2+x_3=0\ . \tag{1.1}$$

The local *period* (or *homological*) coordinates can be defined as integrals of $v=\sqrt{Q}$ over two independent homology cycles on the elliptic curve (the "canonical covering") $\widehat{\mathcal{C}}$ defined by the equation $v^2=Q$ (see Sect. 5.1 for details). The real slice $\mathcal{Q}_0^{\mathbb{R}}(-7)$ of $\mathcal{Q}_0(-7)$ is defined by the requirement that all periods of v are real and then the space $\mathcal{Q}_0^{\mathbb{R}}(-7)$ stratifies into cells of (real) dimensions 2 (the top cell of generic elements), of dimension 1 i.e. the cell where two zeros of Q coincide) and zero dimensional (three coincident roots $x_1=x_2=x_3=0$).

The reality of all periods of v implies that the period σ of the curve $\widehat{\mathcal{C}}$ belongs to a one-dimensional subset $\mathcal{R}_1$ of the modular curve shown in Fig.11, left pane.

The space $\mathcal{Q}_0^{\mathbb{R}}(-7,[1]^3)$ is fibered over the set $\mathcal{R}_1$ with fiber $\mathbb{R}_+$. The points at ∞ of $\mathcal{R}_1$ correspond to the space $\mathcal{Q}_0^{\mathbb{R}}(-7,1,2)$. The point of intersection of $\mathcal{R}_1$ with the real axis in the plane of the J–invariant (Fig.11, right pane) is $J\simeq 940.34$ and it corresponds to the Boutroux–Krichever curve [27, 16, 2], which is the unique Boutroux curve in $\mathcal{Q}_0^{\mathbb{R}}(-7,[1]^3)$ possessing a real involution * which leaves the Jenkins-Strebel differential invariant: $\overline{Q(x^\star)}=Q(x)$.

The zeros x_1, x_2 and x_3 are connected by two horizontal (i.e. parallel to the real line in the plane of coordinate $z(x)=\int^x v$) geodesics in the metric $|Q|$. We will always denote by x_2 the "central" zero which is connected by these geodesics to two others. Then the remaining zeros x_1 and x_3 can also be labeled such that in the positive direction around the origin x_3 goes after x_2 and x_1 after x_3.

The lengths of the two geodesics are given by the absolute values $A=\left|\int_{x_1}^{x_2}\sqrt{Q}\right|$, $B=\left|\int_{x_2}^{x_3}\sqrt{Q}\right|$. The lengths (A,B) define the map of the space $\mathcal{Q}_0^{\mathbb{R}}(-7,[1]^3)$ to $\mathbb{R}_+^2$.

Discriminant circle bundle on $\mathcal{Q}_0^{\mathbb{R}}(-7)$. Consider the section φ_1 of a $U(1)$ bundle over $\mathcal{Q}_0^{\mathbb{R}}(-7)$ given by the argument of the modular discriminant

$$\varphi_1=\mathrm{Arg}\Delta_1 \tag{1.2}$$

where

$$\Delta_1=[(x_1-x_2)(x_3-x_1)(x_3-x_2)]^2. \tag{1.3}$$

Although Δ_1 itself is well-defined only on the stratum $\mathcal{Q}_0^{\mathbb{R}}([1]^3,-7)$, its argument φ_1 can be continued smoothly through the boundaries $A=0$, $B=0$.

We will show (Theorem 2) that then increment of φ_1 on $\mathcal{Q}_0^{\mathbb{R}}(-7)$ between the boundaries $A=0$ and $B=0$ equals $\pi/5$; this computation is technically non-trivial. Therefore, $\pi/5$ is the monodromy of φ_1 around the zero dimensional cell (represented by $Q=x^3\mathrm{d}x^2$) on the space $\mathcal{Q}_0^{\mathbb{R}}(3,-7)$.

Description of $\mathcal{Q}_0^{\mathbb{R}}([-3]^2)$. The complex moduli space $\mathcal{Q}_0([-3]^2)$ consists of quadratic differentials Q on the Riemann sphere with two poles of degree 3. The generic element of this space is represented by

$$Q=\frac{(x-x_1)(x-x_2)}{x^3}(dx)^2\ ,\quad x_1\neq x_2,\quad x_1\neq 0\neq x_2. \tag{1.4}$$

The integrals of $\sqrt{Q}$ along paths two arbitrary independent homology classes on the canonical covering $y^2=x(x-x_1)(x-x_2)$ are local period coordinates on $\mathcal{Q}_0([-3]^2)$.

The space $\mathcal{Q}_0^{\mathbb{R}}([-3]^2)$ is defined by the condition that all periods of $v=\sqrt{Q}$ on $\widehat{\mathcal{C}}$ are real; it is fibered over the set $\mathcal{R}_{-1,-1}$ of real dimension 1 within the modular curve (Fig. 15, left pane) with the fiber $\mathbb{R}_+$.

The points at ∞ of $\mathcal{R}_{-1,-1}$ correspond to the "wall" i.e. to the space $\mathcal{Q}_0^{\mathbb{R}}(2,[-3]^2)$.

The set $\mathcal{R}_{-1,-1}$ intersects the real axis in the plane of the J–invariant at $J\simeq\{-1690,586,7791\}$ (Fig.15, right pane). The points $J\simeq -1690$ and $J\simeq 586$ correspond to curves with a real involution, however the differential Q is not invariant with respect to this involution. The point $J\simeq 7791$ ($x_1\simeq 1.8037,\ \ x_2=-0.3797$) corresponds to a curve possessing a real involution $\star$ (acting as a standard complex conjugation) such that $\overline{Q(x^\star)}=Q(x)$. This is the natural analog of the Boutroux–Krichever curve in the space $\mathcal{Q}_0^{\mathbb{R}}([-3]^2)$.

One of the zeros, which we denote by x_1, is connected by an infinite horizontal geodesics in the metric $|Q|$ to the pole $x=0$, and another zeros (x_2) to the pole $x=\infty$. In this way we get the labeling of the zeros x_1 and x_2 in this case. The zeros x_1 and x_2 are connected by two horizontal geodesics which we denote by e_1 and e_2. The geodesics e_1 and e_2 will be labelled as follows: when one arrives to x_1 along horizontal geodesics emanating from $x=0$, turning right one follows the geodesics e_1, and turning left one follows the geodesics e_2 (see Fig. 7). The length of e_1 will be denoted by A and the length of e_2 by B.

The lengths (A,B) define the map of the space $\mathcal{Q}_0^{\mathbb{R}}([-3]^2,[1]^2)$ to $\mathbb{R}_+^2$.

Discriminant circle bundle on $\mathcal{Q}_0^{\mathbb{R}}([-3]^2)$. The sections $\varphi^{\pm}_{-1,-1}$ of the two natural $U(1)$ bundles over $\mathcal{Q}_0^{\mathbb{R}}([-3]^2)$ are given by the following expressions:

$$\varphi^{\pm}_{-1,-1}=\operatorname{Arg}\Delta^{\pm}_{-1,-1} \tag{1.5}$$

$$\Delta^{+}_{-1,-1}:=x_1^6x_2^6(x_1-x_2)^2,\qquad \Delta^{-}_{-1,-1}:=x_1^6x_2^6(x_1-x_2)^{26}\,. \tag{1.6}$$

The analysis contained in Section 6 shows that the increments of $\varphi^{\pm}_{-1,-1}$ between the boundary $A=0$ and the boundary $B=0$ on $Q_0^{\mathbb{R}}([-3]^2)$ equals 13π and 25π, respectively.

Therefore, monodromies of $\varphi^{\pm}_{-1,-1}$ along a simple closed, non-contractible loop in $\mathcal{Q}_0^{\mathbb{R}}([-3]^2)$ equal 13π and 25π, respectively (see Thm. 4).

In summary, the main results of this paper are the following. First, we show how the moduli spaces $Q_0^{\mathbb{R}}(-7)$ and $Q_0^{\mathbb{R}}([-3]^2)$ appear under a degeneration of a generic Strebel graph via shrinking of two adjacent edges. Second, we study analytically the spaces $Q_0^{\mathbb{R}}(-7)$ and $Q_0^{\mathbb{R}}([-3]^2)$ and natural circle bundles over them. These results provide the analytical tools necessary to apply the formalism of the Bergman tau-function in the description of various tautological classes to the combinatorial model of $\mathcal{M}_{g,n}$ [3].

The paper is organized as follows. In Section 2 we recall the combinatorial model of $\mathcal{M}_{g,n}$ based on Jenkins-Strebel differentials. In section 3 we describe a neighbourhood of Witten's cycle W_1 in the combinatorial model and show how the moduli space $Q_0^{\mathbb{R}}(-7)$ appears in this context. In Section 4 we describe a neighbourhood of Kontsevich's boundary $W_{-1,-1}$ of $\mathcal{M}_{g,n}^{comb}$ and demonstrate the appearance of the space $Q_0^{\mathbb{R}}([-3]^2)$. In Section 5 we study the geometry of the space $Q_0^{\mathbb{R}}(-7)$ in detail and compute the increment of the argument of the modular discriminant Δ_1 on this space. Finally, in Section 6 we study the geometry of the space $Q_0^{\mathbb{R}}([-3]^2)$ and compute the increment of the arguments of $\Delta^{\pm}_{-1,-1}$ on this space.

2 Combinatorial model of $\mathcal{M}_{g,n}$ via Jenkins-Strebel differentials

Here we briefly recall the main ingredients of the combinatorial model of the moduli spaces of Riemann surfaces based on Jenkins-Strebel differentials. The moduli space of Riemann surfaces of genus g with n marked points is denoted by $\mathcal{M}_{g,n}$ and its Deligne-Mumford compactification by $\overline{\mathcal{M}}_{g,n}$. Let $\mathcal{C}$ be a Riemann surface of genus g and Q be a meromorphic quadratic differential with second order poles at the points $y_1,\dots,y_n$. Zeros of Q are denoted by $x_1,\dots,x_m$ and their multiplicities by $\mathbf{d}=(d_1,\dots,d_m)$; we have $\sum_{i=1}^m d_i=4g-4+2n$. Denote by $\mathcal{Q}_{g,n}^{\mathbf{d}}$ the moduli space of such quadratic differentials; its dimension equals $2g-2+n+m$. For the stratum of highest dimension, when all zeros are simple and $m=4g-4+2n$, this dimension equals $6g-6+3n$.

Canonical cover. The equation

$$v^2 = Q$$

in $T^*\mathcal{C}$ defines a two-sheeted covering $\widehat{\mathcal{C}}$ of $\mathcal{C}$, called *canonical covering* in Teichmüller theory ($\widehat{\mathcal{C}}$ is known under the name of "spectral covering" in the theory of Hitchin's systems or under the name of "Seiberg-Witten curve" in the theory of supersymmetric Yang-Mills theory). The branch points of the covering coincide with zeros of odd multiplicity of Q, whose number we denote by m_{odd}: then the genus of the canonical covering is $\hat{g} = 2g + \frac{m_{odd}}{2} - 1$. For a generic Q, which has $4g - 4 + 2n$ simple zeros, $\hat{g} = 4g - 3 + n$. It is convenient to introduce the notation

$$g_- = \hat{g} - g = g + \frac{m_{odd}}{2} - 1$$

Denote by μ the holomorphic involution interchanging the sheets of $\widehat{\mathcal{C}}$. The Abelian differential of the third kind v on $\widehat{\mathcal{C}}$ has $2n$ simple poles at the points $\{y_i, y_i^\mu\}$ (slightly abusing the notations we use y_i to denote positions of poles both on $\mathcal{C}$ and $\widehat{\mathcal{C}}$). Consider the decomposition of $H_1(\widehat{\mathcal{C}} \setminus \{y_i, y_i^\mu\}_{i=1}^n, \mathbb{R})$ (whose dimension equals $2\hat{g} + 2n - 1$) into the direct sum of even and odd subspaces:

$$H_+ \oplus H_- \ , \qquad \dim H_+ = 2g + n - 1, \quad \dim H_- = 2g_- + n. \tag{2.1}$$

Notice that $\dim H_- = \dim \mathcal{Q}^{\mathbf{d}}_{g,n}$. Consequently, one can introduce a system of local coordinates on the space $\mathcal{Q}^{\mathbf{d}}_{g,n}$ called *"homological coordinates"* by choosing a set of independent cycles s_i, $i = 1, \ldots, \dim H_-$ in H_- and integrating v over these cycles:

$$\mathcal{P}_i = \int_{s_i} v \ . \tag{2.2}$$

The following definition of Jenkins-Strebel differential is equivalent to the standard one [25]:

Definition 1 *The quadratic differential Q is called Jenkins-Strebel differential if all homological coordinates $\mathcal{P}_i$ are real.*

The reality of all $\mathcal{P}_i$ implies that the biresidues of Q at its poles y_j are real and negative i.e. there exist such $p_j \in \mathbb{R}_+$ that in any local coordinate ζ near y_j one has:

$$Q(\zeta) = \frac{-(p_j/2\pi)^2}{\zeta^2} \left(1 + \mathcal{O}(\zeta)\right) (\mathrm{d}\zeta)^2 \tag{2.3}$$

Results of Jenking and Strebel provide the existence and uniqueness of a differential Q on a given Riemann surface with n marked points with *given* constants $p_i \in \mathbb{R}_+$ and all *real* periods $\int_{s_i} v$ for $s_i \in H_-$ (combinations of cycles surrounding z_i also form a part of H_-; the reality of periods of v around these cycles is guaranteed by the form of biresidues in (2.3)). This statement provides a basis for the combinatorial description of $\mathcal{M}_{g,n}$.

For each given vector $\mathbf{p} = (p_1, \ldots, p_n) \in \mathbb{R}^n_+$ one can construct a combinatorial model of the moduli space $\mathcal{M}_{g,n}$ which will be denoted by $\mathcal{M}_{g,n}[\mathbf{p}]$. Namely, for each Riemann surface $\mathcal{C}$ of genus g with n marked points $z_1, \ldots, z_n$ consider the unique Jenkins-Strebel differential Q whose singular part at z_i is as in (2.3).

The stratum $\mathcal{M}^{\mathbf{d}}_{g,n}[\mathbf{p}]$ of $\mathcal{M}_{g,n}[\mathbf{p}]$ consists of punctured Riemann surfaces such that the Jenkins-Strebel differential Q has zeros of multiplicities $\mathbf{d} = (d_1, \ldots, d_m)$. The real dimension of the stratum $\mathcal{M}^{\mathbf{d}}_{g,n}[\mathbf{p}]$ is given by

$$\dim_{\mathbb{R}} \mathcal{M}^{\mathbf{d}}_{g,n}[\mathbf{p}] = 2g - 2 + m \tag{2.4}$$

The largest stratum corresponds to Jenkins-Strebel differentials with simple zeros and has real dimension equal to $6g - 6 + 2n$ (in this case $m = 4g - 4 + 2n$) which coincides with the real dimension of $\mathcal{M}_{g,n} \times \mathbb{R}^n_+$.

The oriented horizontal trajectories of the 1-form v on $\widehat{\mathcal{C}}$ (which project down to the non-oriented horizontal trajectories of Q on $\mathcal{C}$) connect zeros x_i.

These horizontal trajectories on $\mathcal{C}$ form the edges of an embedded graph (also called *fatgraph*, or *ribbon graph*) Γ on $\mathcal{C}$ with vertices at $x_1, \ldots, x_m$ and valencies $d_1 + 2, \ldots, d_m + 2$, respectively. Therefore, the stratum of highest dimension $6g - 6 + 2n$ corresponds to fatgraphs on $\mathcal{C}$ with trivalent vertices.

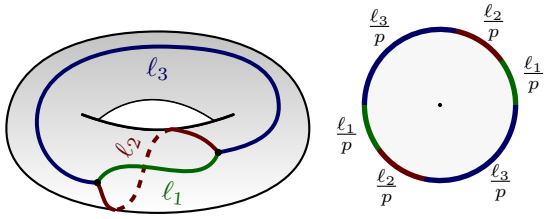

Figure 1: Fatgraph on a genus 1 Riemann surface representing a point in $\mathcal{M}_{1,1}[\mathbf{p}]$. Two simple zeros x_1 and x_2 of Q are connected by 3 edges of lengths ℓ_1, ℓ_2 and ℓ_3. The fatgraph has only one face of perimeter $p = 2(\ell_1 + \ell_2 + \ell_3)$. The lengths ℓ_1 and ℓ_2 can be used as coordinates on $\mathcal{M}_{1,1}[p]$

The length ℓ_e of an edge $e \in E(\Gamma)$ connecting two vertices v_1, v_2 is equal to the absolute value of the integral of v along the horizontal trajectory connecting the two vertices. In turn, up to a factor of $1/2$, this length coincides with the integral of v over the integer cycles in H_- consisting of the trajectory e on one sheet of the projection $\widehat{\mathcal{C}} \to \mathcal{C}$ and the same trajectory in the opposite direction on the other sheet. Fixing the vector $\mathbf{p} \in \mathbb{R}_+^n$ one imposes n linear constraints on the lengths of the edges: for the j–th face $f_j \in F(\Gamma)$, $\quad j = 1, \ldots, n$ we have $\sum_{e \in \partial f_j} \ell_e = p_j$. A simple example of fatgraph on a Riemann surface of genus 1 with one marked point is shown in Fig. 1. In the flat metric $|Q|$ on $\mathcal{C}$ the neighbourhoods of a pole y_i is an infinite cylinder of perimeter p_i.

The union of all strata $\mathcal{M}_{g,n}^{\mathbf{d}}[\mathbf{p}]$ for fixed $\mathbf{p} \in \mathbb{R}_+^n$ forms the combinatorial model $\mathcal{M}_{g,n}[\mathbf{p}]$ of $\mathcal{M}_{g,n}$. This combinatorial model is set-theoretically isomorphic to $\mathcal{M}_{g,n}$.

The compactification $\overline{\mathcal{M}}_{g,n}[\mathbf{p}]$ of the combinatorial model is constructed by addition of the so–called *Kontsevich boundary* to $\mathcal{M}_{g,n}[\mathbf{p}]$: the stratum $W_{-1,-1}$ of real co-dimension 2 of the Kontsevich boundary corresponds to fatgraphs with exactly two one–valent vertices (i.e. two simple poles of the JS differential Q), while all other vertices remain trivalent.

The Kontsevich boundary is "smaller" than the Deligne-Mumford boundary of $\mathcal{M}_{g,n}$ since the Jenkins-Strebel combinatorial model is not applicable to non-punctured Riemann surfaces.

Each face F_j of the fatgraph Γ (the face F_j contains the pole y_j) can be mapped to the unit disk via the map

$$w_j(x) = \exp\left(\frac{2\pi i}{p_j}\int_{x_j}^{x} v\right) \; ; \tag{2.5}$$

where x_j is an arbitrarily chosen vertex of the face F_j. Under the map (2.5) y_j is being mapped to the origin and x_j to 1. One can always choose the branch of the differential $v = \sqrt{Q}$ which has residue $\frac{p_j}{2\pi i}$ at y_j. Within the face F_j the flat metric $|Q| = |v|^2$ on $\mathcal{C}$ is expressed as:

$$|Q| = \frac{p_j^2}{4\pi^2}\left|\frac{dw_j}{w_j}\right|^2 \; . \tag{2.6}$$

The fatgraph corresponding to the stratum of highest dimension in the combinatorial model $\mathcal{M}_{1,1}^{comb}[p]$ shown in Fig. 1 has only one face; this face can be mapped to the unit disk. The constraint between lengths in this case reads $2(\ell_1 + \ell_2 + \ell_3) = p$.

Inverting this logic it is possible to construct a polyhedral Riemann surface (i.e. Riemann surface with flat metric with conical singularities) from a fatgraph equipped with lengths of all edges by the *conformal welding* [25].

All strata of $\mathcal{M}_{g,n}[\mathbf{p}]$ can be obtained from the stratum of highest dimension W (which corresponds to fatgraphs with all tri-valent vertices) by contraction of one or more edges. Various components of W are glued along (real) codimension one boundaries which correspond to fatgraphs with one vertex of valency 4 and all other vertices of valency 3 (i.e. the Jenkins-Strebel differential corresponding to the boundary has one double zero and other zeros are simple). The procedure of crossing the boundary from one cell of W to another

(sometimes in this way one can get into the same cell; then the cell is "wrapped on itself") is described by the so-called Whitehead move shown in Fig.3.

Our goal will be to study in detail the contraction of two edges having one vertex in common. Then depending on geometry one gets either cells forming the Witten's cycle W_1 (corresponding fatgraphs have one 5-valent vertex and other vertices of valency 3), or cells forming the Kontsevich's boundary $W_{-1,-1}$ of $\mathcal{M}_{g,n}[\mathbf{p}]$ (which corresponds to fatgraphs having two vertices of valency 1 and all other vertices of valency 3). These two types of contraction are shown in Fig.2

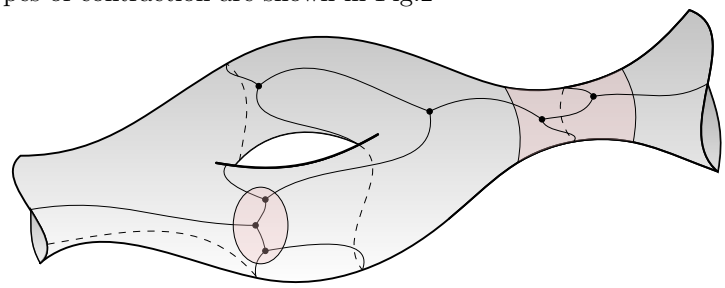

Figure 2: A typical embedded Strebel graph. The two highlighted regions are where the contraction of edges leads either to the cell W_1 (left region) or to the cell $W_{-1,-1}$ (right region).

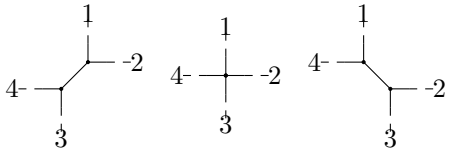

Figure 3: The Whitehead move.

3 A local model near Witten's cycle W_1: the space $Q_0^{\mathbb{R}}(-7)$

Cells of the cycle W_1 in the combinatorial model $\mathcal{M}_{g,n}[\mathbf{p}]$ (the vector $\mathbf{p}$ will be kept fixed in all constructions below) correspond to fatgraphs which have all vertices of valency 3 except one vertex which has valency 5. Here we shall understand an n-punctured Riemann surface $\mathcal{C}$ as an element of the combinatorial model $\mathcal{M}_{g,n}[\mathbf{p}]$ i.e. we assume that $\mathcal{C}$ uniquely defines the JS differential Q.

A point of W_1 can be obtained from a trivalent fatgraph via contraction of two edges having one vertex in common; conversely, any Riemann surface from a neighbourhood of $\mathcal{C}$ in W is a two (real)-parameter deformation of $\mathcal{C}$. We are going to show how this deformation can be described via "flat surgery" of a Riemann surface $\mathcal{C}$ and a Riemann sphere equipped with an appropriate real-normalized quadratic differential. This flat surgery also explicitly gives the Jenkins-Strebel differential and the fatgraph on the deformed Riemann surface.

Furthermore, the flat surgery can also be understood in terms of a "plumbing construction" connecting $\mathcal{C}$ with a Riemann sphere equipped with an appropriate flat metric.

Denote the zero of order 3 of the JS differential on $\mathcal{C}$ by x_1; denote also the fatgraph corresponding to $\mathcal{C}$ by Γ. Let ζ be a "distinguished" local parameter on $\mathcal{C}$ near x_1: $\zeta(x) = \left[\frac{5}{2}\int_{x_1}^{x} v\right]^{2/5}$ ($\zeta(x)$ is defined up to a fifth root of unity); thus $Q(x)$ can be written in terms of ζ as $Q(\zeta) = \zeta^3(\mathrm{d}\zeta)^2$. The local coordinate on the canonical cover $\widehat{\mathcal{C}}$ near x_1 is given by $\zeta^{1/2}$.

Introduce also the "flat" coordinate (both on $\mathcal{C}$ and $\widehat{\mathcal{C}}$):

$$z(x) = \int_{x_1}^{x} v\ ;$$

in a neighbourhood of x_1 the flat coordinate is expressed via the local coordinate ζ as $z = \frac{2}{5}\zeta^{5/2}$. We have $Q(x) = (\mathrm{d}z(x))^2$ on $\mathcal{C}$ and $v = \mathrm{d}z$ on $\widehat{\mathcal{C}}$. The metric $|Q(x)|$ has a conical point at x_1 with cone angle 5π while at all other vertices the cone angle equals 3π.

3.1 Resolution of a 5-valent vertex by flat surgery

There are 5 edges of the fatgraph Γ emanating from the vertex x_1; their directions are given by the angles $\frac{2\pi k}{5}$ in the ζ-plane. Denote their lengths (starting from the edge going along positive real line) by $\ell_1, \ldots, \ell_5$. We are

going to construct an explicit deformation $\mathcal{C}^{\alpha,\beta}$ of $\mathcal{C}$ with two real ("small") parameters, α and β, by changing these lengths as follows:

$$(\ell_1, \dots, \ell_5) \to (\ell_1 - (\alpha+\beta),\, \ell_2 + \beta,\, \ell_3 - \beta,\, \ell_4 - \alpha,\, \ell_5 + \alpha) \tag{3.1}$$

The triple zero, $\widetilde{x}$, of Q on $\mathcal{C}$ splits into three simple zeros (x_1, x_2, x_3) of the JS differential $Q^{\alpha,\beta}$ on $\mathcal{C}^{\alpha,\beta}$. We assume that the new edges of length $\ell_1 - (\alpha+\beta)$ and $\ell_2 + \beta$ meet at x_1; x_1 is connected to x_2 by the edge of length α, x_2 is the endpoint of the edge $\ell_2 + \beta$ and it is also connected to x_3 by the edge of length β; the edges $\ell_4 - \alpha$ and $\ell_5 + \alpha$ meet at x_3. The resulting configuration is shown in Fig.4.

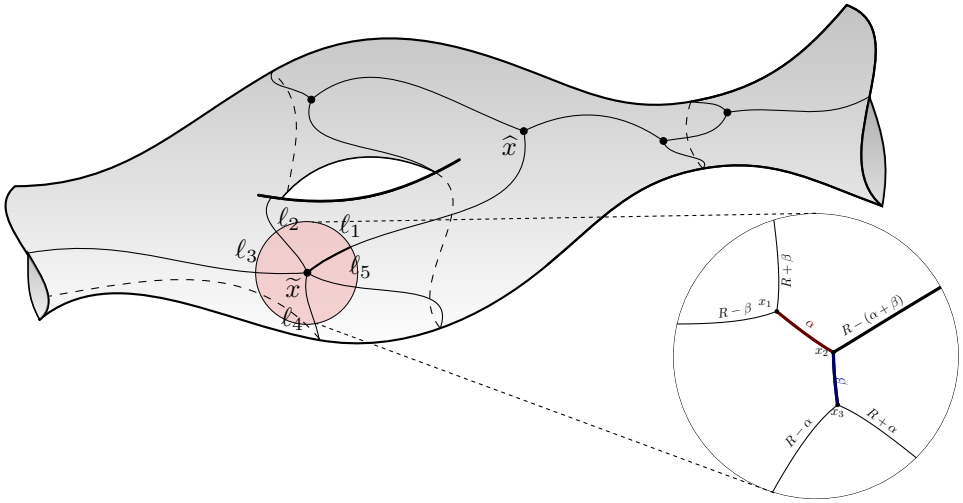

Figure 4: The Riemann surface $\mathcal{C}^{\alpha,\beta}$ is obtained by replacing the five-valent vertex with three regular vertices and two new edges of length α and β between them with appropriate adjustment of the lengths of the original fatgraph. The limit $\alpha, \beta \to 0$ produces the original Riemann surface. The five arcs on the boundaries of the plug-in region are five semicircles or radius R in the flat coordinates of either metrics.

We then construct a two–(real) parameter family $\mathcal{C}^{\alpha,\beta}$ of deformations of $\mathcal{C}$ as explained below.

Fix some radius R which satisfies the conditions $R < \ell_i$ for $i = 1, \dots, 5$. Consider the disk $\mathcal{D}_R$ given by $|z(x)| \le R$ on $\mathcal{C}$ (see Fig. 4); in terms of the coordinate ζ the disk $\mathcal{D}_R$ is given by $|\zeta| \le \left(\frac{5R}{2}\right)^{2/5}$. Five edges of the fatgraph Γ within $\mathcal{D}_R$ are given by the segments $\left[0, \left(\frac{5R}{2}\right)^{\frac{2}{5}}\right] \mathrm{e}^{\frac{2i\pi}{5}k}$, $k = 0, \dots, 4$ in the ζ-plane. The perimeter of $\mathcal{D}_R$ in the flat metric $|Q|$ equals $5\pi R$.

Let us now excise the region $\mathcal{D}_R$ from the Riemann surface $\mathcal{C}$ and obtain a Riemann surface with boundary, which we denote by $\mathcal{C}_R$. Denote by $\widehat{\mathcal{C}}_R$ the canonical cover $\widehat{\mathcal{C}}$ with the disk $\mathcal{D}_R$ deleted on both copies of $\mathcal{C}$. Let us assume that the branch cut connecting the triple zero $\widetilde{x}$ with some other zero on $\mathcal{C}$ (say, $\widehat{x}$) goes along the positive real line in the ζ - coordinate.

We are going to attach to $\widehat{\mathcal{C}}_R$ another disk $\mathcal{D}_R^{\alpha,\beta}$ which we now describe. Consider an element of the moduli space $Q_0^{\mathbb{R}}[-7]$, that is, a quadratic differential Q_0 on $\mathbb{C}P^1$ given by

$$Q_0(x) = (x - x_1)(x - x_2)(x - x_3)\mathrm{d}x^2 \tag{3.2}$$

such that $x_1 + x_2 + x_3 = 0$. The Abelian differential $v_0 = \sqrt{Q_0}$ is defined on the canonical cover $\widehat{\mathcal{C}}_0$ of $\mathbb{C}P^1$ that is the elliptic curve with branch points at x_1, x_2, x_3 and ∞.

Assume that all periods of v_0 on $\widehat{\mathcal{C}}_0$ are real. Then there exist two horizontal trajectories of v_0 on $\mathbb{C}P^1$ which connect x_1, x_2 and x_3. Assume that x_2 is the "central" zero i.e. it is connected by the horizontal trajectories

to x_1 and x_3. Choose the branch cuts on $\widehat{\mathcal{C}}_0$ to connect x_2 with x_1, x_3 and ∞ along the horizontal trajectories. Assume also that x_1 and x_3 are enumerated such tat the branch cuts $[x_2,\infty)$, $[x_2,x_1]$ and $[x_2,x_3]$ meet at x_2 in the counterclockwise order as shown in Fig.5, left (this picture is drawn in the coordinate x).

Introduce on $\widehat{\mathcal{C}}_0$ a canonical basis of cycles (a,b) such that the a-cycle encircles the branch points x_1 and x_2 and b-cycle encircles the branch points x_2 and x_3. The real periods of v_0 over cycles a and b are expressed as follows via the lengths α and β of the branch cuts $[x_2,x_1]$ and $[x_2,x_3]$:

$$\Big|\int_a v_0\Big| = 2\alpha \ , \qquad \Big|\int_b v_0\Big| = 2\beta \ . \tag{3.3}$$

The conditions (3.3) determine the branch points x_i up to multiplication of all x_i by a fifth root of unity (see Th. 1).

The quadratic differential Q_0 which has three simple zeros and one pole of degree 7 on $\mathbb{C}P^1$ is an element of the space $\mathcal{Q}_0^{\mathbb{R}}([1]^3,-7)$; it is an analog of the Jenkins-Strebel differential in the case of a pole having an order higher than 2.

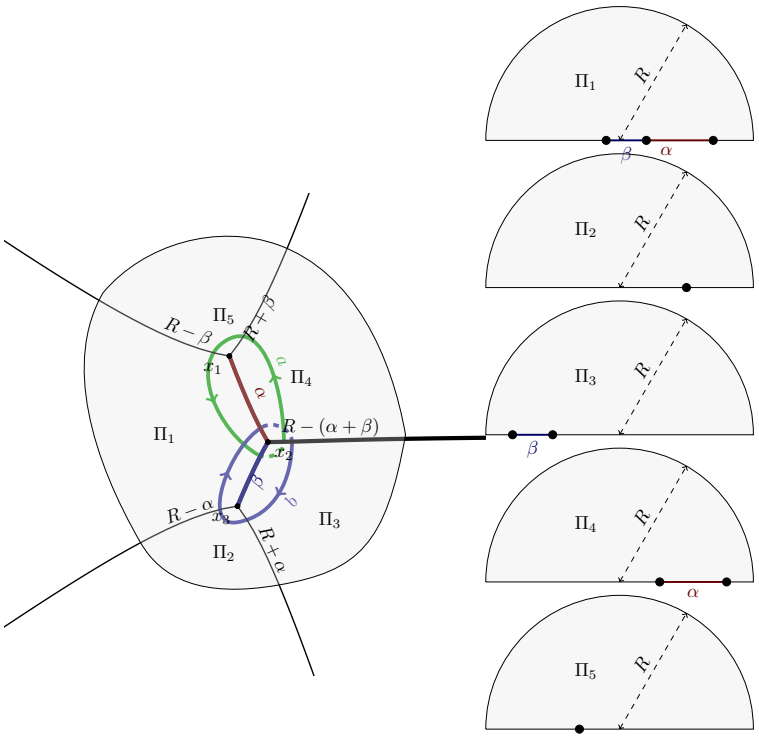

Figure 5: Left: the ribbon graph on $\mathbb{CP}^1$ of the quadratic differential Q_0 and the geodesic disk of radius R drawn in coordinate x. Indicated are the distances in the metric $|Q_0|$ along the trajectories. Right: the five half-disks in the upper half plane, uniformized by the flat coordinate.

We choose the branch cuts to go along the edges $[x_1,x_2]$, $[x_3,x_2]$ and $[x_2,\infty]$ (the thick lines in Fig. 5, left pane). The edges of the fatgraph Γ_0 split the x-plane into 5 regions as shown in Fig.5 (left). Five horizontal trajectories of v_0 which connect x_1, x_2 and x_3 to ∞ approach ∞ along the rays $\arg x = 2\pi k/5$. In the flat metric $|Q_0|$ on $\mathbb{C}P^1$ each of these five regions is uniformized by the flat coordinate z to a half-plane $\operatorname{Im} z > 0$.

On each of the five rays connecting the point at infinity with the points x_i we cut segments whose lengths (starting from the ray $[x_2,\infty)$ and counting couterclockwise) are chosen to be $R-\alpha-\beta$, $R+\beta$, $R-\beta$, $R-\alpha$ and $R+\alpha$. Then we consider a half-circle (in the flat metric $|Q_0|$) in each region which connects the endpoints of the chosen segments (Fig. 5, right). It is easy to see that the diameters of all of these five half-circles coincide and are all equal to $2R$. In this way we obtain five regions which are half-disks of radius R in the flat coordinate z; they will be denoted by $\Pi_1,\dots,\Pi_5$, and their union by $\mathcal{D}_R^{\alpha,\beta}$.

The flat coordinates in each of the regions Π_i are defined up to sign and translations; the global flat coordinate on the whole $\mathcal{D}_R^{\alpha,\beta}$ is defined as follows. Choose the initial point of integration to be x_2 and choose the system

of three branch cuts within $\mathcal{D}_R^{\alpha,\beta}$ as shown in Fig.5 (left): then the flat coordinate on $\mathcal{D}_R^{\alpha,\beta}$ with three deleted branch cuts is defined by

$$w(x) = \alpha + \beta + \int_{x_2}^{x} v_0 \tag{3.4}$$

where the determination of v_0 has to be chosen so that the image of Π_4 is in the upper half plane of the z–variable. One can easily verify that, according to the orientation of the a- and b- cycles on $\mathcal{C}_0$ shown in Fig.5, left pane, the values of the coordinate $w(x)$ on different sides of the branch cut $[x_2, \infty)$ differ by a sign.

The canonical two-sheeted cover of the domain $\mathcal{D}_R^{\alpha,\beta}$ with branch cuts going along horizontal trajectories $[x_2, x_1]$, $[x_2, x_3]$ and $[x_2, \infty)$ will be denoted by $\widehat{\mathcal{D}}_R^{\alpha,\beta}$.

The shape and perimeter of the boundary of $\mathcal{D}_R^{\alpha,\beta}$ in the global flat coordinate is a circle winding by an angle of 5π. The positions of the points where the outgoing edges (in z-coordinate) and the branch cut intersect the boundary of $\mathcal{D}_R^{\alpha,\beta}$, coincide with those of $\mathcal{D}_R$. In particular, the perimeter of $\mathcal{D}_R^{\alpha,\beta}$ also equals $5\pi R$. Therefore, we can identify the boundary of $\mathcal{C}_R$ with the boundary of $\mathcal{D}_R^{\alpha,\beta}$ (this procedure is called "conformal welding" in [25]) to get the new Riemann surface $\mathcal{C}^{\alpha,\beta}$ together with its canonical cover $\widehat{\mathcal{C}}^{\alpha,\beta}$. The five lengths of the edges originally connected to the zero of order 3 on $\mathcal{C}$ are then changed according to (3.1). Notice that this deformation preserves perimeters of all faces of the fatgraph; therefore the Riemann surface $\mathcal{C}^{\alpha,\beta}$ and the corresponding fatgraph belong to the same combinatorial model $\mathcal{M}_{g,n}[\mathbf{p}]$ as the original surface $\mathcal{C}$.

Moreover, the result of such "conformal welding" does not depend on the choice of radius R of the excised disk as long as it remains sufficiently small in comparison with $\ell_1, \ldots, \ell_5$ and sufficiently large in comparison with α and β.

3.2 Plumbing construction

To study the limit $\alpha, \beta \to 0$ in the previous "conformal welding" scheme one needs to degenerate the quadratic differential (3.2) on $\mathbb{C}P^1$. The equivalent "plumbing" construction presented here allows to keep $\mathcal{C}$ and $\mathcal{C}_0$ fixed.

To deform $\mathcal{C}$ into $\mathcal{C}^{\alpha,\beta}$ (and conversely, to study the limit $\alpha, \beta \to 0$ of $\mathcal{C}^{\alpha,\beta}$) we introduce the "plumbing parameter" $t = \alpha + \beta$ and the parameters

$$A = \frac{\alpha}{t} = \frac{\alpha}{\alpha + \beta} \qquad B = \frac{\beta}{t} = \frac{\alpha}{\alpha + \beta} \tag{3.5}$$

such that $A + B = 1$.

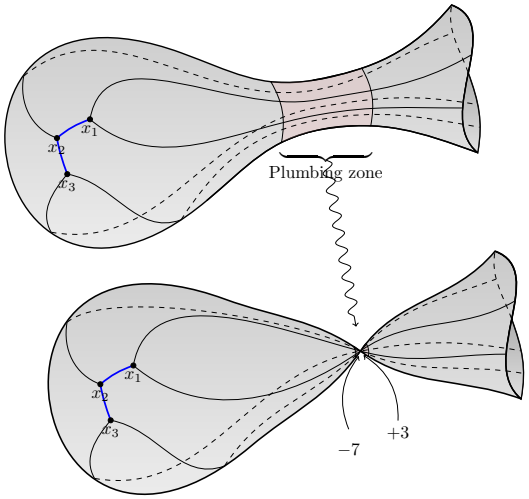

Figure 6: Separating of the Riemann sphere with three simple zeros and a pole of order 7 of Q in a neighbourhood of W_1

Let us now excise from $\mathcal{C}$ a disk $\mathcal{D}_{2t}$ of radius $R = 2t$ with centre at x_1.

To replace this disk we consider quadratic differential Q_0 of the form (3.2) such that the absolute value of the periods of the corresponding Abelian differential v_0 are given by $2A$ and $2B$ (instead of 2α and 2β as before) so that the lengths of the finite edges of the corresponding fatgraph equal A and B.

In parallel to the construction of the previous section we cut from the Riemann sphere the domain $\mathcal{D}_{2/t}^{A,B}$. The radius of the hole of $\mathcal{C} \setminus \mathcal{D}_{2t}$ is $2t$ while the radius of the domain $\mathcal{D}_{2/t}^{A,B}$ equals $2/t$. Therefore, denoting as before the flat coordinate on $\mathcal{C}$ in a neighbourhood of x_1 by z, and the flat coordinate near the boundary of $\mathcal{D}_{2/t}^{A,B}$ by w, one has to identify the boundaries via $\frac{z}{w} = t^2$. However, the distinguished local coordinate near $\widetilde{x}$ on $\mathcal{C}$ (in terms of the flat coordinate $z = \int_{\widetilde{x}}^{x} v$) is $\zeta = \left(\frac{5}{2}z\right)^{2/5}$. On the Riemann sphere side, we consider the local coordinate $\xi(x) = \left[\frac{5}{2}w(x)\right]^{-2/5}$ in terms of the global flat coordinate $w(x) = 1 + \int_{x_2}^{x} v_0$ as in (3.4).

Now, consider on $\mathcal{C} \setminus \mathcal{D}_{2t}$ a small annulus A_ϵ defined by $2t < |z(x)| < 2t + \epsilon$ (with coordinate ζ on A_ϵ). On the Riemann sphere side we consider the annulus A_ϵ^0 defined by $2/t < w(x) < 2/t + \epsilon/t^2$ (with coordinate $\xi(x)$ on A_ϵ^0).

Then the identification of the annuli A_ϵ and A_ϵ^0 which is required by the standard plumbing construction is defined by the relation

$$\xi(x)\zeta(y) = t^{\frac{4}{5}} \tag{3.6}$$

where $x \in A_\epsilon$, $y \in A_\epsilon^0$.

The "plumbing" point of view is illustrated in Fig. 6. We notice the following difference of the present framework with the standard plumbing picture. Usually the plumbing parameter is complex and can be used as a local coordinate near the boundary. In our framework we have two real deformation parameters: one of them is the plumbing parameter, while the second is the ratio $\frac{B}{A} \in [0, \infty]$ which defines the meromorphic differential on the attached Riemann sphere.

4 A local model near Kontsevich's boundary $W_{-1,-1}$ and space $Q_0^{\mathbb{R}}([-3]^2)$

The cells of the main stratum $W_{-1,-1}$ of the Kontsevich boundary of the combinatorial model $\mathcal{M}_{g,n}[\mathbf{p}]$ correspond to fatgraphs which have all vertices of valency 3 except two vertices which have valency 1. The one-valent vertices arise as the result of the normalization of the node. The corresponding Riemann surface $\mathcal{C}$ is a (connected or disconnected) nodal curve which belongs to Deligne-Mumford boundary of $\mathcal{M}_{g,n}$. The JS differential Q on $\mathcal{C}$ has simple poles at both points x_1^0 and x_2^0 obtained by normalization of the nodal point on the curve $\mathcal{C}$. The flat metric $|Q(x)|$ has at x_i^0 conical points with cone angle π.

Let us introduce distinguished local coordinates $\xi_{1,2}$ near $x_{1,2}^0$ such that Q in a neighbourhood of x_i^0 takes the form

$$Q(\xi_i) = \frac{(d\xi_i)^2}{\xi_i} \quad \text{as} \quad x \to x_i^0 \, . \tag{4.1}$$

The points $x_{1,2}^0$ are branch points on the canonical covering $\widehat{\mathcal{C}}$ with distinguished local parameters on $\widehat{\mathcal{C}}$ given by $\hat{\xi}_i = \xi_i^{1/2}$; then near x_i^0 we have $v = 2\mathrm{d}\hat{\xi}_i$. Thus the Abelian differential $v = \sqrt{Q}$ is non-singular and non-vanishing on $\widehat{\mathcal{C}}$ at the points x_i^0. Flat coordinates near the points x_i^0 are given by

$$z_i(x) = \int_{x_i^0}^{x} v = 2\xi_i^{1/2}$$

such that $Q(x) = (dz_i)^2$ near x_i^0. Conversely,

$$\xi_i(x) = \frac{z_i^2}{4}$$

Denote lengths of edges ending at x_1^0 and x_2^0 by l_1 and l_2, respectively. Assume that the branch cuts ending at x_1^0 and x_2^0 go along these edges.

4.1 Resolution of two one-valent vertices by flat surgery

To deform the Riemann surface $\mathcal{C}$ into a Riemann surface $\mathcal{C}^{\alpha,\beta}$ which corresponds to JS differential with all simple zeros we fix some R such that $R < \ell_1$ and $R < \ell_2$. Denote the flat disks around x_i^0 defined by inequality $|z_i(x)| < R$ by $\mathcal{D}_{R,i}$ (denote also $\mathcal{D}_R = \mathcal{D}_{R,1} \cup \mathcal{D}_{R,2}$). Excising the disks $\mathcal{D}_{R,i}$ from $\mathcal{C}$ we get an open Riemann surface $\mathcal{C}_R$ with two holes of perimeter πR in the metric $|Q|$. The canonical covering $\widehat{\mathcal{C}}$ with deleted pre-images of $\mathcal{D}_{R,i}$ turns into 2-sheeted covering $\widehat{\mathcal{C}}_R$ of $\mathcal{C}_R$; $\widehat{\mathcal{C}}_R$ is also an open Riemann surface with two holes.

We are going now to construct a deformation $\mathcal{C}^{\alpha,\beta}$ with two real "small" parameters α and β such that the fatgraph corresponding to $\mathcal{C}^{\alpha,\beta}$ has two 3-valent vertices (i.e. two simple zeros of the JS differential Q) instead of two one-valent vertices x_1^0 and x_2^0.

Under such deformation two new edges of lengths α and β appear while the lengths of edges ℓ_1 and ℓ_2 modify as follows:

$$(\ell_1, \ell_2) \to (\ell_1 - \frac{1}{2}(\alpha+\beta), \ell_2 - \frac{1}{2}(\alpha+\beta)) \tag{4.2}$$

so that the perimeters of both faces containing vertices x_1^0 and x_2^0 remain unchanged.

To construct $C^{\alpha,\beta}$ we are going to attach to $\mathcal{C}_R$ an annulus-type domain which we construct as follows.

Consider a point of $\mathcal{Q}_0^{\mathbb{R}}([1]^2, [-3]^2)$ i.e quadratic differential Q_0 on $\mathbb{C}P^1$ with two poles of order 3 (which we identify with $x = 0$ and $x = \infty$), two simple zeros and all real periods:

$$Q_0(x) = \frac{(x-x_1)(x-x_2)}{x^3}(dx)^2 \tag{4.3}$$

The canonical covering corresponding to the differential Q_0 is the elliptic curve $\widehat{\mathcal{C}}_0$ with branch points at x_1, x_2, 0 and ∞ in x-plane. The meromorphic Abelian differential $v_0 = \sqrt{Q_0}$:

$$v_0 = \frac{\sqrt{(x-x_1)(x-x_2)}}{x^{3/2}}dx \tag{4.4}$$

has second order zeros at x_1 and x_2 and second order poles at 0 and ∞ on the canonical cover.

Assume that the branch cuts are chosen along horizontal geodesics in the metric $|Q_0|$ connecting 0 with x_1 and x_2 with ∞. Approaching x_1 along geodesics coming from $x = 0$ we can either turn left (this edge we denote by e_2) or right (this edge we denote by e_1). The lengths of e_1 and e_2 will be denoted by α and β, respectively.

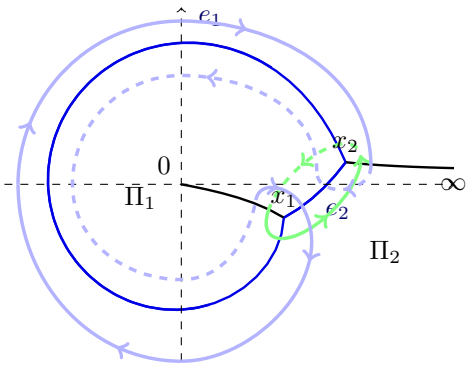

Figure 7: Branch-cuts (black) and other horizontal geodesics (blue) on $\hat{\mathcal{C}}$. Also shown the edges e_1 and e_2.

The flat coordinate on $\mathbb{C}P^1$ and on $\widehat{\mathcal{C}}_0$ is given as usual by the Abelian integral of v_0; the initial point of integration can be chosen arbitrarily (except 0 and ∞). The fatgraph on $\mathbb{C}P^1$ corresponding to Q_0 has two edges of finite lengths α and β which connect points x_1 and x_2 in two different ways, and two edges of

infinite length; we enumerate x_1 and x_2 in such a way that these edges connect 0 with x_1 and ∞ with x_2 (Fig. 7).

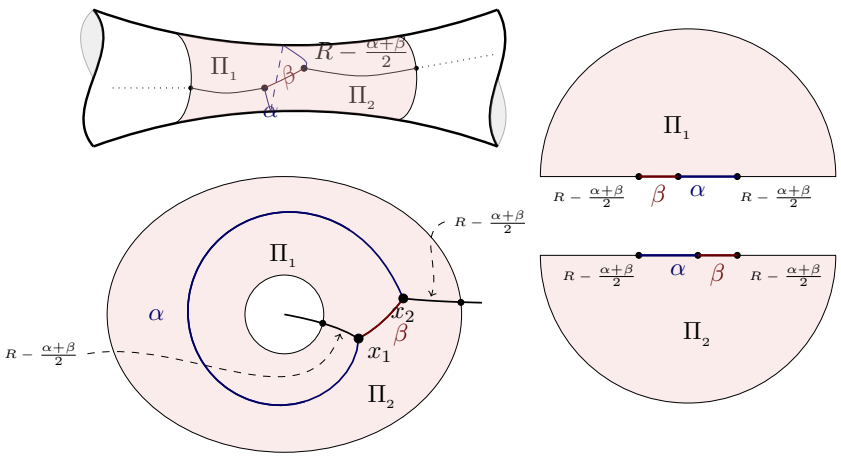

Figure 8: The shaded region in x-plane is conformally mapped to two half-disks in flat coordinate. The trajectories in the x-plane model are numerically accurate.

Consider the annular region $\mathcal{D}_R^{\alpha,\beta}$ which consists of two half-disks Π_1 and Π_2 of radius R in the flat metric $|Q_0|$, glued along segments of length α and β of their diameters to each other (Fig.8). The remaining parts of the diameter of each half–disk (having lengths $R-\frac{\alpha+\beta}{2}$) are glued together on each half-disk separately as shown in Fig.8. The lift $\widehat{\mathcal{D}}_R^{\alpha,\beta}$ of $\mathcal{D}_R^{\alpha,\beta}$ to the canonical covering $\widehat{\mathcal{C}}_0$ has two outgoing branch cuts coinciding with the parts of the diameters of the half-disks of length $R-(\alpha+\beta)/2$. The flat coordinate in Π_1 we given by $z(x)=\int_{x_1}^{x} v$ and the flat coordinate in Π_2 is given by $z(x)=\int_{x_2}^{x} v$; then the boundary of $\mathcal{D}_R^{\alpha,\beta}$ is defined by $|z(x)|=R$.

Perimeters of both boundary components of $\mathcal{D}_R^{\alpha,\beta}$ equal πR in the flat metric $|Q_0|^2$; moreover, both of the boundary components have constant radius R in this metric; the branch cuts go along the real line in flat coordinate. In analogy to the resolution procedure of the 5-valent vertex we "weld" the region $\mathcal{D}_R^{\alpha,\beta}$ to two-holed Riemann surface $\mathcal{C}_R$ such that the branch cuts on $\mathcal{C}_R$ glue with the outgoing branch cuts on $\mathcal{D}_R^{\alpha,\beta}$.

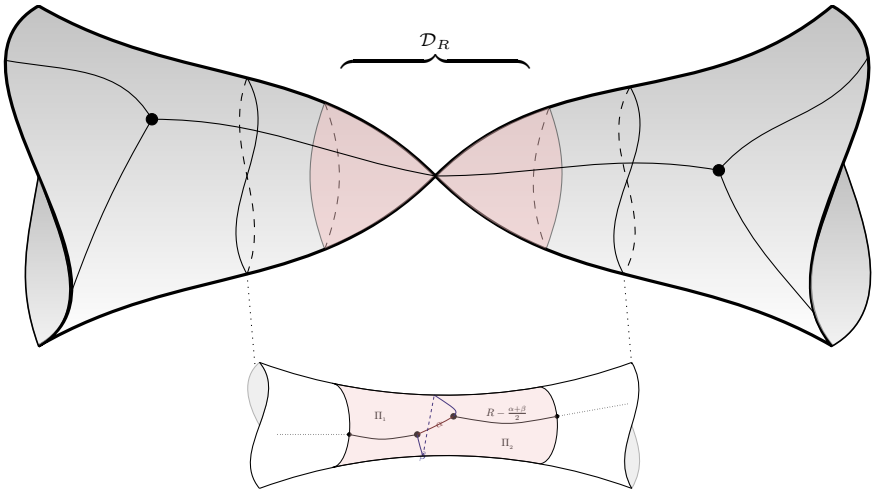

Figure 9: Resolution of a double point $x_{1,2}^0$ on $\mathcal{C}$ by insertion of an annulus with two simple zeros x_1 and x_2

The welding produces the smooth Riemann surface $\mathcal{C}^{\alpha,\beta}$ of genus g. The fatgraph of $\mathcal{C}^{\alpha,\beta}$ is obtained from the fatgraph of $\mathcal{C}$ by replacing edges of lengths ℓ_1 and ℓ_2 on $\mathcal{C}$ by edges of lengths $\ell_i-(\alpha+\beta)/2$ (4.2) and introducing two new edges of lengths α and β. Two one-valent vertices x_1^0 and x_2^0 on $\mathcal{C}$ are then replaced by two trivalent vertices x_1 and x_2 on $\mathcal{C}^{\alpha,\beta}$.

4.2 Plumbing construction

As well as in the case of the the resolution of a point of W_1, to study the limit $\alpha, \beta \to 0$ one needs to consider the degeneration of the quadratic differential (4.3) by taking the limit $x_1, x_2 \to 0$. Alternatively, the "plumbing" construction allows to keep $\mathcal{C}$ and $\mathcal{C}_0$ (together with corresponding JS differentials) fixed while controlling degeneration via the "plumbing parameter" t. The new feature one encounters in the $W_{-1,-1}$ case is the appearance of two plumbing zones instead of one.

To deform $\mathcal{C}$ into $\mathcal{C}^{\alpha,\beta}$ (and vice versa, to study the limit $\alpha, \beta \to 0$ of $\mathcal{C}^{\alpha,\beta}$) we introduce again the plumbing parameter $t = \alpha + \beta$ and define two numbers

$$A = \frac{\alpha}{t} = \frac{\alpha}{\alpha+\beta} \qquad B = \frac{\beta}{t} = \frac{\alpha}{\alpha+\beta} \tag{4.5}$$

such that $A + B = 1$.

As before, construct the surface $\mathcal{C}_R$ by excising two disks of radius $R = 2t$ from $\mathcal{C}$ (in the flat metric $|Q|$) with centers at $x^0_{1,2}$ so that R is smaller than the lengths $\ell_{1,2}$ of the edges of the fatgraph of $\mathcal{C}$ ending at $x^0_{1,2}$.

To replace this disk we consider the quadratic differential Q_0 of the form (4.3) such that the periods of the corresponding Abelian differential v_0 over the cycles $\tilde{a}$ and $\tilde{b}$ shown in Fig. 7 are given by $2A$ and $2B$ (instead of 2α and 2β as before) such that the lengths of the edges connecting x_1 and x_2 of the corresponding fatgraph on $\mathbb{C}P^1$ equal A and B.

Similarly to the construction of the previous section we cut from the Riemann sphere the annular domain $\mathcal{D}^{A,B}_{2/t}$; the lengths of boundaries of $\mathcal{D}^{A,B}_{2/t}$ in the metric $|Q_0|$ equal $2\pi/t$. This time the diameters of the holes of of $\mathcal{C}_{2t}$ differ from diameter of boundaries of $\mathcal{D}^{A,B}_{2/t}$ by the factor of t^2. Denote as before the flat coordinates on $\mathcal{C}$ in neighbourhoods of $x^0_{1,2}$ by $z_{1,2}$.

The flat coordinates near two boundaries of $\mathcal{D}^{A,B}_{2/t}$ are denoted by $w_{1,2}$; these coordinates have to be identified with $t^2 z_{1,2}$. However, the proper local coordinates near $x_{1,2}$ on $\mathcal{C}$ are $\zeta_i = z_i^2/4$. On the other hand, on the Riemann sphere side, we consider the local coordinates $\xi_{1,2}(x) = 4\left[\int_{x_{1,2}}^{x} v_0\right]^{-2}$ near the boundaries of $\mathcal{D}^{A,B}_{2/t}$; the coordinate z_1 is used as a flat coordinate in Π_1 and the coordinate z_2 is used as a flat coordinate in Π_2.

Now, consider on $\mathcal{C}_{2t}$ two small annuli $A_{\epsilon 1,2}$ defined by $2t < z_i(x) < 2t + \epsilon$ (with coordinates ζ_i on $A_{\epsilon 1,2}$). On the Riemann sphere side we consider the annuli $A^0_{\epsilon\,1,2}$ defined by $2/t < w_i(x) < 2/t + \epsilon/t^2$ (with coordinate $\xi(x)$ on A^0_ϵ).

Then the identification of the annuli $A_{\epsilon i}$ and $A^0_{\epsilon\, i}$, required by the standard plumbing construction, is defined by the relation

$$\xi_i(x)\zeta_i(y) = t^4 \tag{4.6}$$

where $x \in A_{\epsilon i}$, $y \in A^0_{\epsilon\, i}$.

The "plumbing" point of view is illustrated in Fig. 10. Again, the difference with the traditional plumbing construction is that the plumbing parameter t is real, while the second deformation parameter B/A is hidden in the moduli of $\mathcal{C}_0$.

5 Modular discriminant Δ_1 on the space $\mathcal{Q}_0^{\mathbb{R}}(-7)$

5.1 Space $\mathcal{Q}_0(-7)$

Stratification. Denote by $\mathcal{Q}_0(-7)$ the complex moduli space of quadratic differentials Q (we omit the index 0 on Q from now on) on $\mathbb{C}P^1$ with one pole of multiplicity 7: the equivalence is that $Q_1 \sim Q_2$ if there exists a Möbius transformation μ such that $\mu^* Q_1 = Q_2$. Therefore, without loss of generality, we can assume that the pole of Q is $x = \infty$; by further shift and rescaling of x the differential Q can be represented as follows

$$Q = (x - x_1)(x - x_2)(x - x_3)(dx)^2 \tag{5.1}$$

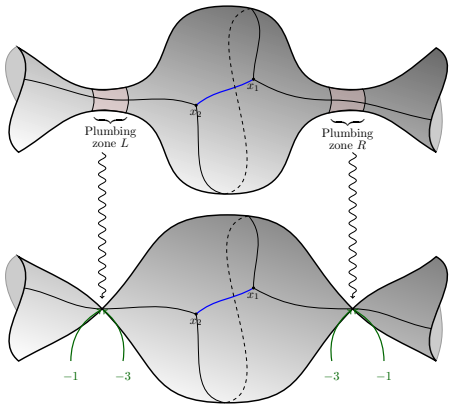

Figure 10: Plumbing construction interpretation of a resolution of a point of Kontsevich's boundary $W_{-1,-1}$: a Riemann sphere with two trivalent and two one-valent vertices is glued between two one-valent vertices by introducing two plumbing zones

where $x_1 + x_2 + x_3 = 0$ and the points are taken up to permutations. We leave it to the reader to verify that differentials of the form (5.1) are equivalent iff the sets of zeros are given by $\{x_i\}$ and $\{\epsilon x_i\}$ where ϵ is the fifth root of unity.

The space $\mathcal{Q}_0(-7)$ has complex dimension two; it can be stratified according to multiplicities of zeros of the quadratic differential Q as follows:

$$\mathcal{Q}_0(-7) = \mathcal{Q}_0(-7,[1]^3) \cup \mathcal{Q}_0(-7,2,1) \cup \mathcal{Q}_0(-7,3) \ . \tag{5.2}$$

Here $\mathcal{Q}_0(-7,[1]^3)$ is the biggest stratum of complex dimension 2; it can be identified with

$$\mathcal{Q}_0(-7,[1]^3) = \{(x_1,x_2,x_3) \in \mathbb{C}^3 \ , \quad x_1+x_2+x_3 = 0 \ , \ \ x_i \neq x_j\}/(S_3 \times \mathbb{Z}_5) \tag{5.3}$$

Consider the canonical cover $\widehat{\mathcal{C}}$ defined by the differential Q:

$$y^2 = (x-x_1)(x-x_2)(x-x_3) \ . \tag{5.4}$$

Introduce on $\widehat{\mathcal{C}}$ some basis of canonical cycles (a,b) and define homological coordinates by integrating the differential $v = y\mathrm{d}x$ over these cycles: $2A = \int_a v$, $2B = \int_b v$. The stratum $\mathcal{Q}_0(-7,2,1)$ coincides with the union of three hyperplanes $x_i = x_j$. Let $x_2 = x_3$ so that $x_1 = -2x_2$. Then, a point of $\mathcal{Q}_0(-7,2,1)$ is represented by a differential of the form

$$Q = (x+2x_2)(x-x_2)^2(dx)^2 \ . \tag{5.5}$$

Finally, the stratum $\mathcal{Q}_0(-7,3)$ contains only one point, represented by the quadratic differential

$$Q = x^3(dx)^2. \tag{5.6}$$

Coordinatization. The periods (A,B) can be used as local coordinates on $\mathcal{Q}_0(-7,[1]^3)$ according to the following lemma:

Lemma 1 *The Jacobian determinant of (A,B) with respect to (x_1,x_2) is given by:*

$$\frac{\partial(A,B)}{\partial(x_1,x_2)} = 2\pi i \Delta_1^{1/2} \tag{5.7}$$

where Δ_1 is the modular discriminant

$$\Delta_1 = [(x_1-x_2)(x_1-x_3)(x_2-x_3)]^2 \tag{5.8}$$

Proof. We have

$$\frac{\partial(A,B)}{\partial(x_1,x_2)} = \oint_a \frac{\partial v}{\partial x_1} \oint_b \frac{\partial v}{\partial x_2} - \oint_b \frac{\partial v}{\partial x_1} \oint_a \frac{\partial v}{\partial x_2} \,. \tag{5.9}$$

To compute this determinant we are going to replace the differential $\partial v/\partial x_1$ by

$$w := \frac{\partial v}{\partial x_1} - \frac{2x_1+x_2}{x_1+2x_2}\frac{\partial v}{\partial x_2} = -\frac{(2x_1+x_2)(x_1-x_2)}{2\sqrt{(x-x_1)(x-x_2)(x-x_3)}}\mathrm{d}x \tag{5.10}$$

which does not change the value of the determinant. Now computation of (5.9) reduces to Riemann bilinear relation between the holomorphic differential w and $\partial v/\partial x_2$ with the only contribution given by the residue at $x=\infty$. This residue is easily computed to give (using $t=\frac{1}{\sqrt{z}}$ as a local parameter near the infinite point):

$$\frac{\partial v}{\partial x_2} = \left(\frac{x_1+2x_2}{t^2} + \mathcal{O}(1)\right)\mathrm{d}t \,;$$

$$w = ((2x_1+x_2)(x_1-x_2) + \mathcal{O}(t))\,\mathrm{d}t \,,$$

which leads to (5.7). ■

The canonical basis (a,b) is defined up to an $SL(2,\mathbb{Z})$ transformation. Thus the periods $(2A,2B)$, as well as the periods $2\omega_1 = \int_a v_0$ and $2\omega_2 = \int_b v_0$ of the holomorphic differential $v_0 = dx/y$, are also defined up to a $SL(2,\mathbb{Z})$ action.

The action of $SL(2,\mathbb{Z})$ on the ratio $\kappa = B/A$ is the same as its action on the period $\sigma = \omega_2/\omega_1$ of the elliptic curve $\mathcal{C}$. In contrast to σ, which always satisfies condition $\operatorname{Im}\sigma > 0$ (in particular ω_1 and ω_2 can not be simultaneously real) no such condition exists for κ.

Associating the period σ of the corresponding canonical cover to the differential Q we get a natural fibration of $\mathcal{Q}_0(-7,[1]^3)$ over the modular curve Ω. The fibre can be identified with $\mathbb{C}^*/\mathbb{Z}_5$ because the $\mathbb{C}^*$–action $(x_1,x_2,x_3)\mapsto(\lambda x_1,\lambda x_2,\lambda x_3)$, $\lambda\in\mathbb{C}^*$, leaves σ invariant but produces generically a new point of $\mathcal{Q}_0(-7,[1]^3)$, unless λ is a fifth root of unity, $\lambda^5=1$.

5.2 Real slice $\mathcal{Q}_0^{\mathbb{R}}(-7)$: Boutroux curves

Elliptic curves corresponding to real periods of the differential v are known as Boutroux curves [4, 6].

The space $\mathcal{Q}_0^{\mathbb{R}}(-7)$ is the real slice of $\mathcal{Q}_0(-7)$ where all the strata are subsets of the corresponding strata of $\mathcal{Q}_0(-7)$ determined by the condition that all periods of $v = y\mathrm{d}x$ on the elliptic curve $v^2=Q$ are real. Thus, the space is stratified as follows:

$$\mathcal{Q}_0^{\mathbb{R}}(-7) = \underbrace{\mathcal{Q}_0^{\mathbb{R}}(-7,[1]^3)}_{\dim_{\mathbb{R}}=2} \sqcup \underbrace{\mathcal{Q}_0^{\mathbb{R}}(-7,2,1)}_{\dim_{\mathbb{R}}=1} \sqcup \underbrace{\mathcal{Q}_0^{\mathbb{R}}(-7,3)}_{\dim_{\mathbb{R}}=0} \tag{5.11}$$

Since $\mathcal{Q}_0(-7,3)$ consists of only one point, we have $\mathcal{Q}_0^{\mathbb{R}}(-7,3) = \mathcal{Q}_0(-7,3)$.

We start from the following lemma describing the configurations of branch points of Boutroux curves:

Lemma 2 ($\mathbb{Z}_5$ and $\mathbb{R}_+$ action) *Suppose that $v = \sqrt{(x-x_1)(x-x_2)(x-x_3)}\mathrm{d}x$, $x_1+x_2+x_3=0$ has all real periods. Then so do the differentials*

$$\sqrt{(x-\mathrm{e}^{\frac{2i\pi k}{5}}x_1)(x-\mathrm{e}^{\frac{2i\pi k}{5}}x_2)(x-\mathrm{e}^{\frac{2i\pi k}{5}}x_3)}\mathrm{d}x \,, \qquad k=1,\dots,4 \tag{5.12}$$

and

$$\sqrt{(x-\lambda x_1)(x-\lambda x_2)(x-\lambda x_3)}\mathrm{d}x \,, \qquad \lambda\in\mathbb{R}_+. \tag{5.13}$$

Proof. Under the map $x_i\mapsto \lambda \mathrm{e}^{\frac{2i\pi k}{5}}x_i$, $i=1,2,3$ the periods transform as $P\mapsto \lambda^{\frac{5}{2}}\mathrm{e}^{i\pi k}P$. Hence under this map the periods are $\mathbb{R}$-scaled but remain real. ■

Lemma 3 **[1]** *If $Q \in \mathcal{Q}_0^{\mathbb{R}}(-7,[1]^3)$ then x_1, x_2 and x_3 do not lie on the same line through the origin in the x-plane.*
[2] *If $Q \in \mathcal{Q}_0^{\mathbb{R}}(-7,2,1)$ then* $\arg x_{1,2} = \left\{\frac{2i\pi k}{5},\ k=0,\dots 4\right\}$ *and* $\arg x_3 = \arg x_{1,2} + \pi$.

Proof. **[1]** Let us show that the assumption that all x_i lie on the same line $\mathrm{e}^{i\theta}\mathbb{R}$ is incompatible with the reality of all periods of v. Using an $\mathbb{R}_+$-rescaling one can assume without loss of generality that $x_1 = \mathrm{e}^{i\theta}$, $x_2 = \lambda x_1$ and therefore $x_3 = -(1+\lambda)x_1$ with some $\lambda > 1$. Then the periods of v are given by the integrals

$$\oint_\gamma v = \mathrm{e}^{\frac{5}{2}i\theta} \oint_\gamma \sqrt{(\tilde{x}-1)(\tilde{x}-\lambda)(\tilde{x}+1+\lambda)}\mathrm{d}\tilde{x}\ , \tag{5.14}$$

where γ is an arbitrary cycle going around the branch points 1, λ and $-1-\lambda$ in the $\tilde{x}$-plane. The integral around the cut $[1,\lambda]$ in (5.14) is imaginary and the integral around the interval $[-1-\lambda,1]$ is real. Thus there is no such value of θ that both of these periods are simultaneously real unless some of the branch points coincide. When some of the branch points coincide, say, $\lambda = 1$, then the reality of the expression $\mathrm{e}^{\frac{5}{2}i\theta}\int_{-2}^{1}(\tilde{x}-1)\sqrt{(\tilde{x}+2)}\mathrm{d}\tilde{x}$ implies $\frac{5}{2}\theta = 0 \bmod \pi$, which proves part **[2]**. ■

Lemma 4 *Let $Q \in \mathcal{Q}_0^{\mathbb{R}}(-7,2,1)$ so that the double root lies on one of the rays $\mathrm{e}^{\frac{2i\pi k}{5}}\mathbb{R}_+$. Then, for any infinitesimal deformation of Q preserving the Boutroux condition, the double root splits into two roots along one of the two directions forming an angle $\pm\frac{\pi}{4}$ with the ray $\mathrm{e}^{\frac{2i\pi k}{5}}\mathbb{R}_+$; the central root emerges along the direction $\pm\frac{5}{4}\pi$, with the angle measured from the ray $\mathrm{e}^{\frac{2i\pi k}{5}}\mathbb{R}_+$ with the positive orientation.*

Proof. Denote by $x_{2,3}$ the two zeroes emerging from the double zero and denote by A the period of v along a small cycle encircling them. Using the $\mathbb{Z}_5$ action (Lemma 2) we can assume without loss of generality that if $x_2 = x_3$ then $\arg x_{2,3} = 2\pi/5$ and $\arg x_1 = 7\pi/5$. To compute the limit of $\arg(x_3 - x_2)$ as $x_3 \to x_2$ we proceed as follows. Let $x_3 = x_2 + \delta$, and $x_1 = -2x_2 - \delta$ where $x_2(\delta) = x_0 + \mathcal{O}(\delta)$ for some $x_0 = |x_0|e^{2\pi i/5}$. Then, up to higher order powers of δ,

$$A = \pm\int_{x_2}^{x_2+\delta}[(x-x_2)(x-x_2-\delta)(x+2x_2+\delta)]^{1/2}\mathrm{d}x$$

$$\sim \pm(3x_0)^{1/2}\int_{x_0}^{x_0+\delta}[(x-x_0)(x-x_0-\delta)]^{1/2}\mathrm{d}x = \pm(-3x_0)^{1/2}\delta^2$$

Therefore, since $A \in \mathbb{R}$ and $\arg(x_0) = 2\pi/5$, we must have (as $\delta \to 0$)

$$2\arg\delta + \frac{\pi}{2} + \frac{\pi}{5} \to 0 \pmod{\pi}$$

and, hence $\arg\delta \to \frac{2\pi}{5} \pm \frac{\pi}{4}$ as $\delta \to 0$. This proves the first assertion.

To prove the second assertion we need to analyze the critical trajectories emerging from $x_{2,3}$ for small δ. To this end we define

$$\zeta = \mathrm{e}^{-\frac{2i\pi}{5}}\frac{(x-|x_0|)}{|\delta|}, \qquad q(\zeta;|\delta|) = |\delta|^{-4}Q(x) \tag{5.15}$$

so that x_2, x_3 are mapped to two points at distance 1 from the origin of the ζ–plane, whereas x_1 is mapped to a point at distance $\mathcal{O}(\delta^{-1})$ from the origin (see Fig. 14). Then, a straightforward computation yields

$$q(\zeta;|\delta|) = (|\delta|\zeta + 3r)\left(\zeta^2 - \mathrm{e}^{2i\arg\delta - \frac{4i\pi}{5}}\right)\mathrm{d}\zeta^2\ . \tag{5.16}$$

Note that q is also quadratic differential with real periods and its trajectory structure has the same topology as the trajectory structure of Q (up to an affine transformation). The ray $\mathrm{e}^{\frac{2i\pi}{5}}\mathbb{R}_+$ is mapped to the positive real axis of the ζ–plane. Now, as $|\delta| \to 0$ (i.e. $A \to 0$) we obtain (uniformly over compact sets in the ζ–plane)

$$\lim_{A\to 0_+} q(\zeta;|\delta|) = 3r(\zeta^2 \pm i)\mathrm{d}\zeta^2\ . \tag{5.17}$$

Consider the case $-i$ in the above expression, the $+i$ case being treated similarly. A simple analysis of the structure of geodesics in the metric given by the modulus of the quadratic differential (5.17) shows that the trajectory that extends to $\mathrm{Re}\,\zeta = -\infty$ issues from $\mathrm{e}^{\frac{5i\pi}{4}}$ (see Fig. 14). Thus the central zero x_2 is the one that is mapped to $\mathrm{e}^{\frac{5i\pi}{4}}$. Similarly for the case $-$. ■

The reality of the periods of v on $\widehat{\mathcal{C}}$ allows to connect x_1, x_2 and x_3 by two horizontal trajectories of the differential v. Then one of the zeros (say, x_2) is connected to x_1 and x_3 and will be referred to henceforth as the *central zero*. Two other zeros x_3 and x_1 will be labeled according to values of their arguments: counterclockwise with respect to the origin we assume that $\arg x_2 < \arg x_3 < \arg x_1$.

All periods of v are real. In addition, it turns out to be convenient to work with positive numbers; thus we introduce an additional modulus in the real setting and define

$$A = \Big| \int_{x_2}^{x_3} v \Big| \,; \qquad B = \Big| \int_{x_2}^{x_1} v \Big| \tag{5.18}$$

where the integration contours go along the horizontal trajectories of v and correspond to $a/2$ and $b/2$ in homologies. Therefore, A and B are the lengths of horizontal geodesics connecting x_2 with x_3 and x_1, respectively.

The flat coordinate $z(x)$ is defined on $\widehat{\mathcal{C}}$ by integration of v with initial point x_2:

$$z(x) = \int_{x_2}^{x} v \tag{5.19}$$

with the branch cuts chosen as the union of trajectories $[x_2, \infty)$, $[x_1, x_2]$ and $[x_2, x_3]$.

The following theorem is an analog of Strebel's theorem which allows to reproduce a Riemann surface with punctures knowing the lengths of edges and topology of the corresponding fatgraph.

Theorem 1 **[1]** *The ordered pair of lengths (A, B) (5.18) defines a one-to-one map of the space $\mathcal{Q}_0^{\mathbb{R}}(-7, [1]^3)$ to $\mathbb{R}_+^2$.*
[2] *The diagonal $A = B$ corresponds to Boutroux curves with an antiholomorphic involution (the* Boutroux-Krichever locus*). By the $\mathbb{Z}_5$ action of Lemma 2, the central zero x_2 of a Boutroux-Krichever curve can always be assumed to be real and positive while the other zeros form a conjugated pair: $x_1 = \bar{x_3}$.*
[3] *The boundaries $A = 0$ and $B = 0$, being identified, correspond to points of the space $\mathcal{Q}_0^{\mathbb{R}}(-7, 2, 1)$. The remaining non-vanishing length parametrizes $\mathcal{Q}_0^{\mathbb{R}}(-7, 2, 1)$.*

Proof. **[1]** The Jacobian of coordinates (A, B) on $\widehat{\mathcal{Q}}_0^{\mathbb{R}}(-7, [1]^3)$ defined by (5.18) never vanishes according to (5.7); however this is not sufficient to prove that a given function of two variables is globally one-to-one. To prove the invertibility we need to restore the triple (x_1, x_2, x_3) uniquely (up to the $\mathbb{Z}_5$ action) from the knowledge of the periods A and B (5.18). Knowing the lengths A and B of the critical graph we construct a polyhedral surface (i.e. surface with flat metric and conical singularities) by gluing 5 half-planes as shown in Fig.5. This uniquely defines the conformal structure i.e J-invariant of $\widehat{\mathcal{C}}$. Moreover, since the zero x_2 is assumed to be "central" and the zeros x_1 and x_3 are labeled we can choose a distinguished pair of canonical a- and b-cycles by assuming that a encircles the critical trajectory connecting x_2 and x_3. Moreover, we fix the direction of the a-cycle such that $A = \frac{1}{2}\int_a v$. The b-cycle then encircles the critical trajectory connecting x_2 and x_1, with an appropriate orientation. This determines the period σ of $\widehat{\mathcal{C}}$ corresponding to such distinguished Torelli marking. In turn, this allows to express the cross-ratio of the points x_i in terms of corresponding theta-constants by the use of Thomæ formulas. We call this ratio t:

$$\frac{x_2 - x_1}{x_3 - x_1} = t \tag{5.20}$$

Introducing the new variable $\tilde{x} = \frac{x - x_1}{x_3 - x_1}$ we can rewrite the first of the equations (5.18) as follows:

$$(x_3 - x_1)^{5/2} \int_t^1 \sqrt{\tilde{x}(\tilde{x} - 1)(\tilde{x} - t)}\, d\tilde{x} = A \tag{5.21}$$

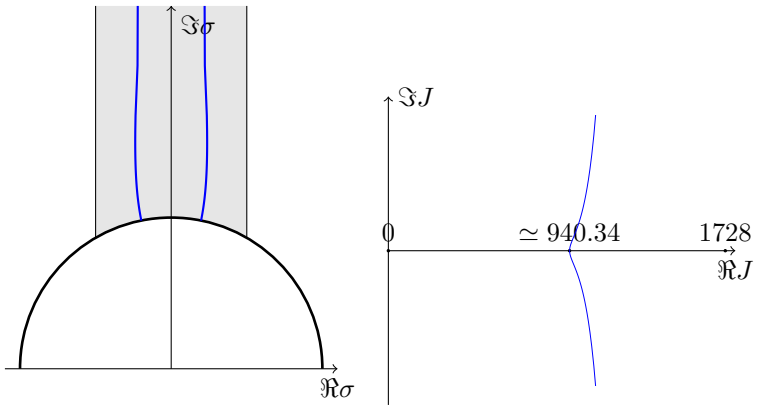

Figure 11: Left: The space of Boutroux curves $\mathcal{Q}_0^{\mathbb{R}}(-7)$ is fibered over the shown curve $\mathcal{R}_1$ in the moduli space of elliptic curves with fiber $\mathbb{R}_+$. Right: the set $\mathcal{R}_1$ in the plane of J-invariant. The point $J = 1728$ corresponds to $\sigma = i$ while $\sigma = e^{2\pi i/3}$ corresponds to $J = 0$. Note that 1728 is the year the English astronomer James Bradley gave the first (and amazingly precise!) estimate of the speed of light.

which implies the relation between x_1 and x_3

$$x_3 - x_1 = \left[\frac{A}{\int_t^1 \sqrt{\tilde{x}(\tilde{x}-1)(\tilde{x}-t)}d\tilde{x}} \right]^{2/5} \tag{5.22}$$

where the right-hand side is known up to a power of $e^{4\pi i/5}$. This allows us to conclude that the system of three linear equations (5.20), (5.22) and $x_1 + x_2 + x_3 = 0$ define all x_i uniquely up to the $\mathbb{Z}_5$ action, which proves that the period map provides an isomorphism between the space $\widehat{\mathcal{Q}}_0^{\mathbb{R}}(-7, [1]^3)$ and the first quadrant in the (A, B)-plane.

[2] Let $A = B$. Then the elliptic curve C admits an anti-holomorphic involution τ which acts as $z \to \bar{z}$ in the flat coordinate z such that the differential $v = \mathrm{d}z$ satisfies the relation $\overline{v(x^\tau)} = v(x)$. The involution τ must act in the x-plane as reflection with respect to some line passing through the origin (since $x_1 + x_2 + x_3 = 0$ and also $x = \infty$ must be invariant under τ); thus τ must interchange x_1 and x_3 while leaving x_2 invariant (all x_i can not be invariant under this involution since they don't lie on the same line as per Lemma 3, item [1]).

Therefore, there exists a real θ such that $x_i = e^{i\theta}x_i'$ while $\overline{x_1'} = x_3'$ and $x_2' \in \mathbb{R}$. Making the change of variable $x = e^{i\theta}x'$ we see that τ acts on x' as $x'^\tau = \bar{x}'$; thus $\tau(x) = e^{-2i\theta}\bar{x}$. Then

$$Q(x) = (x - e^{i\theta}x_1')(x - e^{i\theta}\bar{x}_1')(x - e^{i\theta}x_2')(dx)^2$$

and

$$\overline{Q(x^\tau)} = e^{10i\theta}Q(x)$$

Since we have assumed that not only Q, but also $v = \mathrm{d}z = \sqrt{Q}$ satisfies the relation $\overline{v(x^\tau)} = v(x)$ then 5θ must be a multiple of 2π. Moreover, since we assumed that for non-degenerate curves $0 \le \arg x_2 < 2\pi/5$ we conclude that $x_2 \in \mathbb{R}_+$ and $x_3 = \bar{x}_1$.

[3] Consider a point of $\mathcal{Q}_0^{\mathbb{R}}(-7, 2, 1)$ where, say, $x_2 = x_3 = r\mathrm{e}^{\frac{2i\pi}{5}}$ and $x_1 = -2r\mathrm{e}^{\frac{2i\pi}{5}}$. Then the remaining non-vanishing period B is explicitly computable:

$$B = \left| \int_{x_2}^{x_1} (x - r\mathrm{e}^{\frac{2i\pi}{5}})\sqrt{x - 2r\mathrm{e}^{-\frac{3i\pi}{5}}}\,\mathrm{d}x \right| = \left| \int_{-2r}^{r} (r - z)\sqrt{z + 2r}\,\mathrm{d}z \right| = \frac{12\sqrt{3}}{5} r^{\frac{5}{2}} . \tag{5.23}$$

This shows that the period $B \in \mathbb{R}_+$ is a global coordinate on $\mathcal{Q}_0^{\mathbb{R}}(-7, 2, 1)$. ■

The J-invariant of Boutroux curves traces the curve $\mathcal{R}_1$, computed numerically and shown in Fig.11 (right). The point of intersection of $\mathcal{R}_1$ with the real J–line corresponds to the only curve which is simultaneously real (i.e. it admits an anti-holomorphic involution) and Boutroux. For this curve (known as of Boutroux-Krichever [27]) the J-invariant is approximately given by 940.34. The values of x_i corresponding to this curve are given by

$$x_1 = -1 - 6.492i\,, \qquad x_2 = 2\,, \qquad x_3 = -1 + 6.492i \tag{5.24}$$

(or any multiple of these values with a positive real constant). The set $\mathcal{R}_1$ in the plane of the period σ of the curve $\mathbb{C}$ is shown in Figure 11 (left).

Let us discuss now which configurations of zeros (x_1, x_2, x_3) correspond to a given pair of periods (A, B). The following Proposition provides the converse to certain statements of Lemma 3 and Thm. 1.

Proposition 1 *Suppose that $v = \sqrt{(x-x_1)(x-x_2)(x-x_3)}\mathrm{d}x$, $x_1 + x_2 + x_3 = 0$ has all real periods. Then one of the roots x_i belongs to one of the rays $\mathrm{e}^{\frac{2i\pi k}{5}}\mathbb{R}_+$ iff either*

1. *x_i is a double root (i.e. the curve is degenerate) or;*
2. *the curve is nondegenerate and admits an anti-holomorphic involution exchanging the other two roots, i.e. $\widehat{\mathcal{C}}$ is the Boutroux-Krichever curve of Thm. 1 (point [2]). In this case x_i is the central zero, which we denote by x_2.*

Proof. *Part "⇐".* Suppose that the curve is Boutroux-Krichever. Then the central zero belongs to one of the rays $\mathrm{e}^{\frac{2i\pi k}{5}}\mathbb{R}_+$ by Thm. 1, item [2]. Suppose the curve is degenerate. Write the differential as $v = (x-x_2)\sqrt{x+2x_2}\mathrm{d}x$. Then a direct computation gives $\int_{x_2}^{-2x_2} v = \frac{12\sqrt{3}}{5}x_2^{\frac{5}{2}}$, and this is real iff x_2 belongs to one of the rays.

Part "⇒". Using the $\mathbb{Z}_5$ action and $\mathbb{R}_+$ - scaling of Lemma 2, we can assume that the root in question is $x_j = 2$. Then the other two roots (since the sum is zero) must be of the form $-1 \pm \rho$, for some $\rho \in \mathbb{C}$. Let us write

$$v = \sqrt{(x-2)\,(x+1+\rho)\,(x+1-\rho)}\,. \tag{5.25}$$

The curve is degenerate when $\rho = 0, \pm 3$. The case $\rho = 0$ is excluded since the periods are not real. In both cases $\rho = \pm 3$ the periods are real.

Let now the curve be non-degenerate: it is our goal to show that $\rho \in i\mathbb{R}$, which would also imply that $x_j = x_2 = 2$ is the central root.

To find out for which values of $\rho \neq 0, \pm 3$ both periods are real consider the integrals

$$A_\pm(\rho) = \int_2^{-1\pm\rho} v\mathrm{d}x \tag{5.26}$$

such that that $A_-(\rho) = A_+(-\rho)$. To prove the theorem it is sufficient to show that there is only one solution of the system

$$\mathrm{Im}\, A_+(\rho) = \mathrm{Im}\, A_-(\rho) = 0 \tag{5.27}$$

in the upper half plane and this solution is located on $\mathrm{Re}\,\rho = 0$. The function $A_+(\rho)$ is analytic on the domain $\mathcal{D}_+ = \mathbb{C} \setminus (-\infty, 0]$ while $A_-(\rho)$ is analytic on the domain $\mathcal{D}_- = \mathbb{C} \setminus [0, \infty)$ and both satisfy the Schwartz symmetry $\overline{A_\pm(\overline{\rho})} = A_\pm(\rho)$. The logic of the proof is as follows:

1. Consider the curve (which may consist of several components) $\Phi = 0$, with $\Phi = \mathrm{Im}\, A_+(\rho)$; the solutions of the system (5.27) lie at the intersection of the two curves $\{\Phi = 0\}$ and $-\{\Phi = 0\}$. Taking into account the Schwartz symmetry of the functions $A_\pm(\rho)$ it is sufficient to analyze the upper half plane.

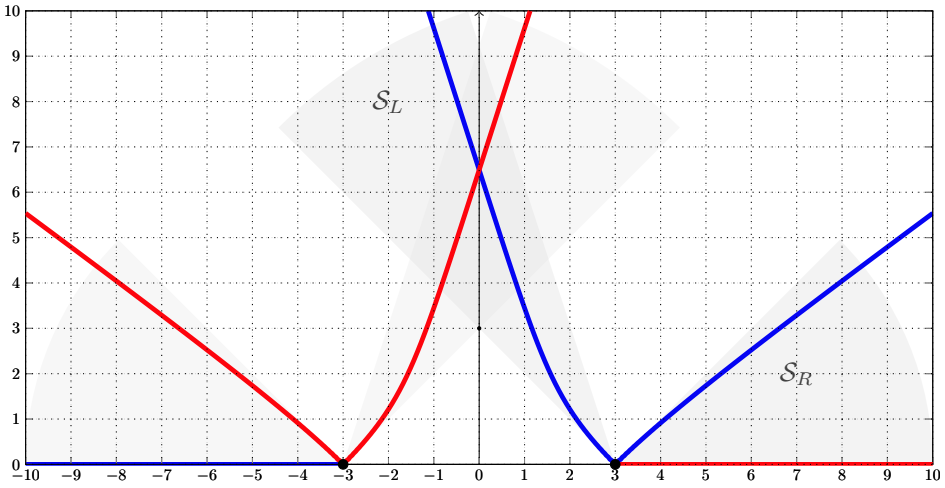

Figure 12: The zero level sets of $\mathrm{Im}\,(A_+(\rho))$ (blue) and $\mathrm{Im}\,(A_-(\rho))$ (red), plotted numerically.

2. Restricting ourselves to the upper half-plane we show that the set $\Phi = 0$ is contained in the union of two sectors, $\mathcal{S}_R$ and $\mathcal{S}_L$ (shown in grey in Fig. 12) which are defined as follows:

$$\{\rho:\ \Phi(\rho)=0\} \subset \underbrace{\left\{\arg(\rho-3)\in\left[\frac{3\pi}{5},\frac{3\pi}{4}\right]\right\}}_{\mathcal{S}_L} \cup \underbrace{\left\{\arg(\rho-3)\in\left[0,\frac{\pi}{4}\right]\right\}}_{\mathcal{S}_R} \tag{5.28}$$

and each of the two sectors contains exactly one smooth branch of the set $\Phi = 0$ starting from $\rho = 3$.

3. Since $\mathcal{S}_L \cap (-\overline{\mathcal{S}_L}) = \emptyset = \mathcal{S}_R \cap (-\overline{\mathcal{S}_L}) = (-\overline{\mathcal{S}_R}) \cap \mathcal{S}_L$, all solutions of (5.27) must lie in $\mathcal{S}_L \cap (-\overline{\mathcal{S}_L})$ (the diamond shaped region in Fig. 12).

4. Show that there is only one point of intersection of $\Phi = 0$ with the positive imaginary axis, and this point lies within the diamond region.

5. Finally, prove that within $\mathcal{S}_L$ the branch of the $\Phi = 0$ is a function of $y = \mathrm{Im}\,\rho$ by showing that no tangent of the foliation $\Phi =$constant can be horizontal within $\mathcal{S}_L$. Together with the previous item this immediately implies the uniqueness of the solution of (5.27).

Let us now discuss these items in more detail.

The item **(1.)** is self-evident. Let us look at item **(2.)** Parametrizing the integral by $x = 2 + (\rho-3)\frac{1-s}{1+s}$, $s \in [0,1]$ we obtain the integral

$$A_+(\rho) = i(\rho-3)^2 \int_0^1 \sqrt{\rho+3s}\,\frac{\sqrt{s(1-s^2)}}{(1+s)^4}\mathrm{d}s \tag{5.29}$$

$$= i(\rho-3)^{\frac{5}{2}} \int_0^1 \sqrt{1+3\frac{s+1}{\rho-3}}\,\frac{\sqrt{s(1-s^2)}}{(1+s)^4}\mathrm{d}s\,. \tag{5.30}$$

From representation (5.30) we see that for $|\rho| \to +\infty$ the four branches have slopes $\pm\frac{\pi}{5}, \pm\frac{3\pi}{5}$. Moreover, there is a fifth branch consisting of the ray $\rho \in (-\infty, -3]$ (the integral is purely imaginary and hence the expression (5.30) is real) but this fifth branch does not play a role in this discussion.

The representation (5.30) is also useful in analysing the argument of A_+ in the finite region; to this end, let us consider this argument for $\mathrm{Im}\,\rho > 0$;

$$\arg(A_+(\rho)) = \frac{\pi}{2} + \frac{5}{2}\arg(\rho-3) + \arg\left(\int_0^1 \sqrt{1+3\frac{s+1}{\rho-3}}\,\frac{\sqrt{s(1-s^2)}}{(1+s)^4}\mathrm{d}s\right)\,. \tag{5.31}$$

It is our goal to see where the argument of A_+ can be equal to 0 or π; if the last term in (5.31) were absent then the set $\Phi = 0$ would simply consist of the rays $\arg(\rho-3) \in \left\{\frac{3\pi}{5}, \frac{\pi}{5}\right\}$. Observing that integrals with positive integration measures preserve cones, we estimate the last term in (5.31) to belong to the interval $(-\frac{\arg(\rho-3)}{2}, 0)$. From (5.31) and the estimate of the argument of the integral we have

$$\frac{\pi}{2} + 2\arg(\rho-3) < \arg A_+(\rho) < \frac{\pi}{2} + \frac{5}{2}\arg(\rho-3). \tag{5.32}$$

To obtain the sectors $\mathcal{S}_{L,R}$ one has to check that in the complement of those sectors the argument of $A_+(\rho)$ cannot be equal to 0 or π. For example in the sector $\arg(\rho-3) \in \left[\frac{\pi}{4}, \frac{3\pi}{5}\right]$ lying between $\mathcal{S}_L$ and $\mathcal{S}_R$ we obtain from (5.32) that $\pi < \arg A_+ < 2\pi$ and hence A_+ cannot be real there. Similarly, in the sector $\arg(\rho-3) \in \left[\frac{3\pi}{4}, \pi\right]$ we have $2\pi < \arg A_+ < 3\pi$, and thus A_+ cannot be real there as well. To summarize:

$$\text{the set } \Phi = 0 \text{ i.e. } \arg A_+(\rho) \in \{0, \pi\} \text{ lies in the union of two sectors, } \mathcal{S}_L \text{ and } \mathcal{S}_R \quad (5.28). \tag{5.33}$$

(see Fig. 12). Moreover, in each of the two sectors there is exactly one branch of the curve $\Phi = 0$ that extends from $\rho = 3$ to infinity; this statement holds since the level sets of harmonic functions cannot form bounded curves unless they surround a singularity; meanwhile $A_+(\rho)$ is harmonic in the whole upper half plane. Moreover, expression (5.29) near $\rho = 3$ shows that there are four branches of $\Phi = 0$ issuing from $\rho = 3$ with slopes $\pm\frac{\pi}{4} \pm \pi$. This proves point **(2.)** and hence also **(3.)**.

Therefore, all solutions to the system (5.27) lie in the diamond–shaped region of intersection $(-\overline{\mathcal{S}_L}) \cap \mathcal{S}_L$ (see Fig. 12). This region lies in the half-plane $\operatorname{Im}\rho \geq 3$.

(4.) Let us now show that the set $\Phi = 0$ for $\operatorname{Im}\rho > 3$ intersects the imaginary ρ–axis $i\mathbb{R}_+$ exactly once at some $\rho = i\rho_\star$. This means that for $\operatorname{Im}\rho < \rho_\star$ the set $\Phi = 0$ lies entirely in the right half-plane, while the branch in $\mathcal{S}_L$ for $\operatorname{Im}\rho > \rho_\star$ lies entirely in the left half-plane. In other words the branch of interest does not "zig-zag" intersecting $i\mathbb{R}_+$ several times.

To this end, let us write out $A_+(iy)$ more explicitly

$$\Phi(iy) = \operatorname{Im} A_+(iy)\ , \quad A_+(iy) = -i(iy-3)^2 \int_0^1 \sqrt{3s+iy}\mathrm{d}\mu(s)\,, \quad \mathrm{d}\mu(s) = \frac{\sqrt{s(1-s^2)}}{(1+s)^4}\mathrm{d}s\ . \tag{5.34}$$

Then

$$\Phi(3i) = \operatorname{Im}\left(-9i(i-1)^2 \int_0^1 \sqrt{3s+3i}\,\mathrm{d}\mu(s)\right) = -18\int_0^1 \operatorname{Im}\left(\sqrt{3s+3i}\right)\mathrm{d}\mu(s) < 0 \tag{5.35}$$

(the approximate value is $\Phi(3i) \simeq -2.2438$). Moreover, for $y \to +\infty$ we have $\Phi(iy) \sim y^{\frac{5}{2}}\frac{\sqrt{2}}{2}\int_0^1 \mathrm{d}\mu(s) \to +\infty$ so that there is at least one solution $\Phi(iy) = 0$ for $y \in [3, \infty)$.

To show uniqueness of this solution suppose that there are several solutions of (5.27) lying on the imaginary axis; at each of these points both $A_\pm$ are real. Then for each of these points we would have $A = B$ and each would give some Krichever–Boutroux curve. But we know from Thm. $1_{[2]}$ that the Krichever–Boutroux curve is unique (up to scaling, which has already been used to set the central root at 2) which leads to a contradiction.

(5.) Let us study the slopes of the tangent vectors to the level curves and show that their tangent can never be horizontal; in other words here we show that within $\mathcal{S}_L$ the argument of $\frac{\mathrm{d}A_+}{\mathrm{d}\rho}$ never equals 0 or π. To this end we analyze the argument of the expression

$$\begin{aligned}\frac{\mathrm{d}A_+(\rho)}{\mathrm{d}\rho} = \oint \frac{\mathrm{d}v}{\mathrm{d}\rho}\mathrm{d}z = i\rho(\rho-3)\int_0^1 \frac{t\mathrm{d}t}{\sqrt{t(1-t^2)\left(\rho+3\frac{1-t}{t+1}\right)}} = \\ = -i\rho(\rho-3)\int_0^1 \frac{1}{\sqrt{\rho+3s}}\frac{(1-s)\mathrm{d}s}{(s+1)\sqrt{s(1-s^2)}}\end{aligned} \tag{5.36}$$

in the sector $S_L = \left\{\arg(\rho-3) \in \left[\frac{3\pi}{5}, \frac{3\pi}{4}\right]\right\}$. To determine the slopes of the curve $\Phi = 0$ we consider $\arg(\mathrm{d}A_+/\mathrm{d}\rho)$ modulo π (i.e. up to sign). Again, we use the fact that an integral with positive measure preserves cones: observe

that, $\forall s \in [0,1], \rho \in S_L$ the following inequalities hold

$$\arg(\rho+3) < \arg(\rho+3s) < \arg(\rho) < \arg(\rho-3) \quad \Rightarrow \quad -\arg(\rho) < -\arg(\rho+3s) < -\arg(\rho+3) \tag{5.37}$$

$$\Rightarrow -\frac{\arg(\rho)}{2} < \arg\left(\int_0^1 \frac{1}{\sqrt{\rho+3s}} \frac{(1-s)\mathrm{d}s}{(s+1)\sqrt{s(1-s^2)}}\right) < -\frac{\arg(\rho+3)}{2} \,. \tag{5.38}$$

Taking into account (5.36) and the above estimates, we find the lower bound

$$\arg\frac{\mathrm{d}A_+}{\mathrm{d}\rho} > -\frac{\pi}{2} + \overbrace{\frac{1}{2}\arg\rho}^{\geq 0} + \overbrace{\arg(\rho-3)}^{\geq \frac{3\pi}{5}} \geq \frac{\pi}{10} \,. \tag{5.39}$$

Likewise, we can obtain an upper bound as follows:

$$\arg\frac{\mathrm{d}A_+}{\mathrm{d}\rho} < -\frac{\pi}{2} + \overbrace{\arg(\rho)}^{<\arg(\rho-3)} \overbrace{-\frac{\arg(\rho+3)}{2}}^{<0} + \arg(\rho-3) < -\frac{\pi}{2} + 2\overbrace{\arg(\rho-3)}^{\leq \frac{3\pi}{4}} \leq \pi \,. \tag{5.40}$$

The cone $\frac{\pi}{10} < \arg(\mathrm{d}A_+/\mathrm{d}\rho) < \pi$ does not contain the real axis, and hence the tangents of our level curves cannot be horizontal. Thus we can parametrize the level curves of $\Phi = 0$ within the sector $\mathcal{S}_L$ by the imaginary part, and point **(5.)** is proved. ■

Assume now that $A \leq B$, the opposite case can be treated symmetrically. Using the $\mathbb{Z}_5$ action (Lemma 2) we arrange so that the central zero x_2 lies in the sector $0 < \arg x_2 \leq \frac{2\pi}{5}$. The following lemma describes the range of argument of x_1 and x_3 under this assumption:

Lemma 5 *Let the argument of central zero x_2 lie in the range*

$$0 \leq \arg x_2 < \frac{2\pi}{5} \tag{5.41}$$

and the zeros x_1 and x_3 be labelled such that $A < B$ (i.e. the distance from x_2 to x_1 is greater than the distance from x_2 to x_3 in the metric $|Q|$). Then the zeros $x_{1,3}$ lie in the following sectors $\mathcal{S}_1$ and $\mathcal{S}_3$ (see Fig 13):

$$\frac{6\pi}{5} \leq \arg x_1 \leq \frac{8\pi}{5} \,, \qquad \frac{2\pi}{5} < \arg x_3 \leq \frac{4\pi}{5} \tag{5.42}$$

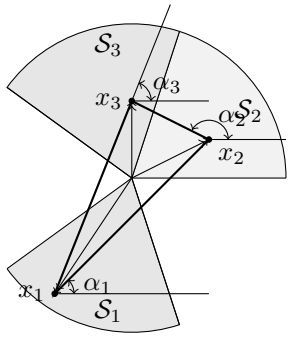

Figure 13

Proof. The proof uses a continuity argument and the statement of Prop. 1. Using the scaling $\mathbb{R}_+$ action, we shall assume $A + B = 1$ throughout this lemma, without loss of generality.

Consider $A = 0, B = 1$; then Prop. 1 implies that $x_3 = x_2$ lie on one of the rays $\mathrm{e}^{\frac{2i\pi k}{5}}\mathbb{R}_+$. Using the $\mathbb{Z}_5$ action (Lemma 2) we can assume $k = 1$ (see Fig. 5.41). As A increases, the two roots $x_2 = x_3$ separate along direction that was computed in Lemma 4 and implies that they move in the two adjacent sectors. We consider the case when the central zero x_2 moves into the sector $(0, \frac{2\pi}{5})$; this corresponds to the case "$-$" in (5.17) (the other case corresponds to a different cell).

For small A we thus know that $x_{1,2,3}$ are in the respective sectors as Fig. 5.41; however, as A increases ($A + B = 1$), we know from Prop. 1 that none of the roots can cross the rays $\mathrm{e}^{\frac{2i\pi k}{5}}\mathbb{R}_+$ unless it is the central zero (which happens only for $A = B$) , or the curve degenerates (when $A = 0$ or $B = 0$). Thus, necessarily the three roots $x_{1,2,3}$ remain in the indicated sectors. ■

5.3 Variation of $\arg\Delta_1$ on $\mathcal{Q}_0^{\mathbb{R}}(-7)$

The goal of this section is to study the variation of the argument of the modular discriminant Δ_1 (5.8) on the moduli space $\mathcal{Q}_0^{\mathbb{R}}(-7)$.

The argument of Δ_1 (5.8) does not change under simultaneous multiplication of all x_i with a positive real constant. Therefore, $\arg\Delta_1$ is constant along any ray passing through the origin in the first octant of the (A,B)-plane. In particular, $\arg\Delta_1$ is constant on each of the rays $A=0$, $B=0$ and $A=B$.

Lemma 6 *Let as before the argument of the central zero x_2 lies between 0 and $2\pi/5$.*

1. *As $A\to 0$ the arguments of x_i-x_j behave as follows:*

$$\arg(x_3-x_2)\to\frac{13\pi}{20}\ ,\qquad \arg(x_3-x_1)\to\frac{2\pi}{5}\ ,\qquad \arg(x_2-x_1)\to\frac{2\pi}{5}\ ;\qquad \arg\Delta_1\to\frac{29\pi}{10} \tag{5.43}$$

2. *As $A=B$ we have*

$$\arg(x_3-x_2)=\pi-\alpha\ ,\qquad \arg(x_3-x_1)=\frac{\pi}{2}\ ,\qquad \arg(x_2-x_1)=\alpha\ ;\qquad \arg\Delta_1=3\pi \tag{5.44}$$

   where α is the angle (lying between 0 and $\pi/2$) formed by the line connecting x_2 and x_3 with horizontal line.

3. *As $B\to 0$ the arguments of x_i-x_j behave as follows:*

$$\arg(x_3-x_2)\to\frac{3\pi}{5}\ ,\qquad \arg(x_3-x_1)\to\frac{3\pi}{5}\ ,\qquad \arg(x_2-x_1)\to\frac{7\pi}{20}\ ;\qquad \arg\Delta_1\to\frac{31\pi}{10} \tag{5.45}$$

Proof. The limits (5.44) are trivial: they follow from the symmetry $x_1=\bar{x}_3$ when $A=B$ and $x_2\in\mathbb{R}$; this proves point [2].

[1], [3]. Consider the limits (5.43) arising as $A\to 0$, when $x_2\to x_3$. When $x_2=x_3$ we have $\arg x_{2,3}=2\pi/5$ and $\arg x_1=7\pi/5$; since all x_i lie on the line going through the origin, we have in this case $\arg(x_{2,3}-x_1)=2\pi/5$.

The angles formed by the tangent directions of $x_{2,3}$ in the process of resolution of a double zero have been computed in Lemma 4: it follows from it that the limit of $\arg(x_3-x_2)$ as $x_3\to x_2$ is

$$\lim_{A\to 0}\arg(x_3-x_2) \;=\; \frac{2\pi}{5}+\frac{\pi}{4}=\frac{13\pi}{20} \tag{5.46}$$

$$\lim_{A\to 0}\arg(x_3-x_1) \;=\; \lim_{A\to 0}\arg(x_2-x_1)=\frac{2\pi}{5}. \tag{5.47}$$

and hence

$$\arg\Delta_1=\lim_{A\to 0}2\arg\big((x_2-x_1)(x_3-x_1)(x_3-x_2)\big)=\frac{13\pi}{10}+\frac{8\pi}{5}=\frac{29\pi}{10}. \tag{5.48}$$

The proof of (5.45) proceeds then in a similar fashion. ■

We now are in a position to state the first main analytical result:

Theorem 2 *The variation of $\varphi_1=\arg\Delta_1$ on the space $\mathcal{Q}_0^{\mathbb{R}}(-7)$ from the boundary $B=0$ to the boundary $A=0$ equals $\pi/5$. In other words, the monodromy of φ_1 around the point $Q=x^3dx$ of $\mathcal{Q}_0^{\mathbb{R}}(-7)$, equals $\pi/5$.*

Proof. almost immediately follows from Lemma 6. To confirm that no additional multiple of 2π arises when one computes such variation it is sufficient to observe that, according to positions of x_1 and x_3, when $\arg x_2$ is bounded between 0 and $2\pi/5$ (Fig. (13)) the following inequalities hold:

$$\pi/5\le\arg(x_3-x_1)\le 4\pi/5\qquad 2\pi/5\le\arg(x_3-x_2)\le\pi\qquad 0\le\arg(x_2-x_1)\le 3\pi/5$$

which confirms that the variation of $\arg\Delta_1$ between the boundary $A=0$ and the diagonal $A=B$ indeed equals $\pi/10$; thus the variation of $\arg\Delta_1$ between the boundaries $A=0$ and $B=0$ equals $\pi/5$. ■

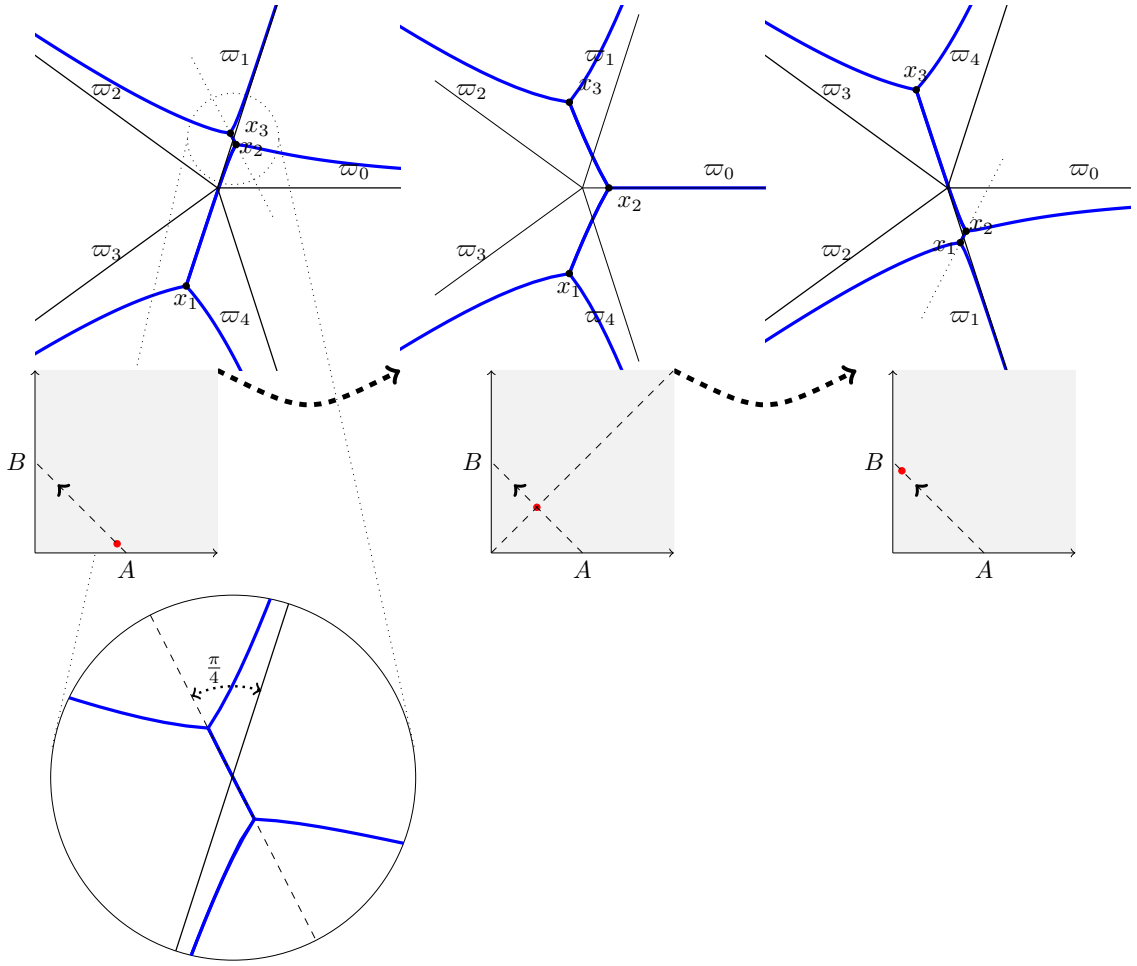

Figure 14: The motion of the roots $\{x_i\}$ as the periods (A, B) traverse a cell from $(0, 1)$ to $(1, 0)$ along $A+B = 1$. The zoom-in inset shows the angle of approach of the roots x_1 and x_3 to the ray $\arg x = 2\pi/5$ as $(A, B) \to (0, 1)$.

6 Arguments of $\Delta^{\pm}_{-1,-1}$ on the space $\mathcal{Q}^{\mathbb{R}}_0([-3]^2)$

In this section we study the space $\mathcal{Q}^{\mathbb{R}}_0([-3]^2)$ which represents a local model of Kontsevich's boundary $W_{-1,-1}$ of the Strebel combinatorial model of $\mathcal{M}_{g,n}$. We compute the monodromy of the argument of $\Delta^{+}_{-1,-1} = x_1^6 x_2^6 (x_1 - x_2)^2$ and $\Delta^{-}_{-1,-1} = x_1^6 x_2^6 (x_1 - x_2)^{26}$ which are the natural analogs of the modular discriminant on $Q^{\mathbb{R}}_0([-3]^2)$. The motivation for studying these expressions comes from the theory of Bergman tau-functions $\tau_{\pm}$ on the spaces of quadratic differentials [19, 15].

6.1 Space $Q_0([-3]^2)$

An element of the space $\mathcal{Q}_0([-3]^2)$ is a quadratic differentials Q on the Riemann sphere with two poles of degree 3 each. The complex dimension of $\mathcal{Q}_0([-3]^2)$ equals 2 and it is stratified as follows:

$$\mathcal{Q}_0([-3]^2) = \mathcal{Q}_0([-3]^2, [1]^2) \sqcup \mathcal{Q}_0([-3]^2, 2) \tag{6.1}$$

Using a Möbius transformation we can assume that the two poles are $x = 0$ and $x = \infty$; the remaining

freedom of rescaling of Q allows us to represent it as follows:

$$Q = \frac{(x-x_1)(x-x_2)}{x^3}(dx)^2 \tag{6.2}$$

where $x_1 \neq x_2$ are two complex parameters.

Therefore we can identify $\mathcal{Q}_0([-3]^2,[1]^2)$ with the space:

$$\mathcal{Q}_0([-3]^2,[1]^2) \simeq \left\{(x_1,x_2\right\} \in (\mathbb{C}^*)^2, \quad x_1 \neq x_2\left\}/S_2 \tag{6.3}$$

For any $Q \in \mathcal{Q}_0([-3]^2,[1]^2)$ we introduce the canonical cover $\widehat{\mathcal{C}}$ defined by $v^2 = Q$; this is the elliptic curve $y^2 = x(x-x_1)(x-x_2)$ endowed with the meromorphic differential

$$v = \sqrt{\frac{(x-x_1)(x-x_2)}{x^3}}dx \tag{6.4}$$

having zeros of second order on $\widehat{\mathcal{C}}$ at x_1, x_2 and poles of second order at $x = 0$ and $x = \infty$.

Choosing two canonical cycles (a,b) on $\widehat{\mathcal{C}}$ and integrating the differential v over cycles a and b we get periods A and B which are defined up to $SL(2,\mathbb{Z})$ transformation as usual.

According to the next lemma, the periods (A,B) can be used as local coordinates on $\mathcal{Q}_0([-3]^2,[1]^2)$:

Lemma 7 *The Jacobian of change of variables from (x_1,x_2) to (A,B) is given by the following formula:*

$$\frac{\partial(A,B)}{\partial(x_1,x_2)} = \pm 2\pi i \frac{x_1-x_2}{x_1x_2} \tag{6.5}$$

Proof. The proof is similar to the proof of (5.7). Namely, to compute the determinant

$$\frac{\partial(A,B)}{\partial(x_1,x_2)} = \oint_a \frac{\partial v}{\partial x_1}\oint_b \frac{\partial v}{\partial x_2} - \oint_b \frac{\partial v}{\partial x_1}\oint_a \frac{\partial v}{\partial x_2} \tag{6.6}$$

with

$$\frac{\partial v}{\partial x_1} = -\frac{1}{2}\frac{1}{x^{3/2}}\left(\frac{x-x_2}{x-x_1}\right)^{1/2}, \qquad \frac{\partial v}{\partial x_2} = -\frac{1}{2}\frac{1}{x^{3/2}}\left(\frac{x-x_1}{x-x_2}\right)^{1/2} \tag{6.7}$$

we replace the differential $\partial v/\partial x_1$ by the holomorphic differential

$$w = \frac{\partial v}{\partial x_1} - \frac{b}{a}\frac{\partial v}{\partial x_2} = \frac{x_2-x_1}{2x_1}\frac{\mathrm{d}x}{[x(x-x_1)(x-x_2)]^{1/2}} \tag{6.8}$$

(this transformation does not change the determinant). Then (6.6) can be computed by applying Riemann bilinear relations to the holomorphic differential w and the meromorphic differential $\frac{\partial v}{\partial x_2}$ which has a pole of order 2 at $x = 0$. The computation of residue of $\left(\int^x w\right)\frac{\partial v}{\partial x_2}$ at $x = 0$ in the local parameter $\sqrt{x}$ gives $(x_1x_2)^{-1}(x_1-x_2)$ which leads to (6.5). ■

6.2 Real slice $Q_0^{\mathbb{R}}([-3]^2)$: Boutroux curves

By $Q_0^{\mathbb{R}}([-3]^2)$ we denote the space of "Boutroux curves" i.e. the real slice of $Q_0([-3]^2)$ where all periods of $v = \sqrt{Q}$ are real. The stratification of $\mathcal{Q}_0^{\mathbb{R}}([-3]^2)$ is:

$$\mathcal{Q}_0^{\mathbb{R}}([-3]^2) = \mathcal{Q}_0^{\mathbb{R}}([-3]^2,[1]^2) \cup \mathcal{Q}_0^{\mathbb{R}}([-3]^2,2)\ ,$$

where the stratum $\mathbb{Q}_0^{\mathbb{R}}([1]^2,[-3]^2)$ has real dimension 2 and the stratum $\mathcal{Q}_0^{\mathbb{R}}([-3]^2,2)$ has real dimension one. The latter corresponds to differentials $v = x^{-3/2}(x-x_1)dx$ such that their period $\int_{x_1^{(1)}}^{x_1^{(2)}} v = 8x_1^{1/2}$ is real (here $x_1^{(1)}$ and $x_1^{(2)}$ are points on different sheets of Riemann surface of function $x^{1/2}$ having projection x_1 on x-plane), i.e. $x_1 \in \mathbb{R}_+$.

To define periods of v we consider horizontal trajectories of v which look as shown in Fig.7: two horizontal geodesics always connect x_1 and x_2 while two other trajectories connect one of the zeros (labelled x_1) to $x = 0$ and another zero (labelled x_2) to $x = \infty$. We label the geodesics as follows. Let e_0 is the horizontal trajectory connecting $x = 0$ to x_1. When we arrive to x_1 following e_0 we denote by e_1 the first counterclockwise horizontal trajectory issuing from x_1 and by e_2 the remaining one; both e_1 and e_2 end at x_2. Denote the length of e_1 (in the metric $|Q|$) by A and the length of e_2 by B (Fig.7).

Theorem 3 *The ordered pair of lengths (A, B) defines a one-to-one map between the space $\mathcal{Q}_0^{\mathbb{R}}([1]^2, [-3]^2)$ and $\mathbb{R}^2_+$. The boundaries $A = 0$ and $B = 0$ of $\mathbb{R}^2_+$ are identified and coincide with the space $\mathcal{Q}_0^{\mathbb{R}}([-3]^2, 2)$. The remaining period defines a one-to-one map of the space $\mathcal{Q}_0^{\mathbb{R}}([-3]^2, 2)$ to $\mathbb{R}_+$.*

The set $A = B$ corresponds to real curves, when $x_{1,2} \in \mathbb{R}$ (the numerical analysis show that for these curves the approximate value of J-invariant equals $J \sim 7791$).

Proof. To prove that the period map is invertible on $\widehat{\mathcal{Q}}_0^{\mathbb{R}}([-3]^2, [1]^2)$ we need to restore the pair (x_1, x_2) uniquely knowing periods A and B. The lengths A and B of the critical graph define a polyhedral surface (i.e. surface with flat metric and conical singularities) by gluing 2 half-planes as shown in Fig.8. This uniquely defines the conformal structure i.e J-invariant of $\widehat{\mathcal{C}}$. Moreover, since the labeling of x_1 and x_2 is fixed, we uniquely reproduce the ratio $t = x_1/x_2$.

Let us choose the canonical a-cycle on $\widehat{\mathcal{C}}$ such that $2A = \int_a v$. Then the definition of the period

$$2A = \int_\alpha \left[\frac{(x - x_1)(x - x_2)}{x^3}\right]^{1/2} \mathrm{d}x$$

can be after the substitution $\tilde{x} = x/x_2$ written as

$$2A = x_2^{1/2} \int_1^t \left[\frac{(\tilde{x} - t)(\tilde{x} - 1)}{\tilde{x}^3}\right]^{1/2} \mathrm{d}\tilde{x}$$

which fixes x_2 uniquely since t is already known.

This proves the isomorphism between $\mathcal{Q}_0^{\mathbb{R}}([-3]^2, [1]^2)$ and the first quadrant $\mathbb{R}^2_+$ in (A, B)-plane. ■

The periods σ of canonical coverings $\widehat{\mathcal{C}}$ corresponding to points of $\mathcal{Q}_0^{\mathbb{R}}([-3]^2, [1]^2)$ span the one-dimensional subset $\mathcal{R}_{1,1}$ of the moduli space $\mathcal{M}_1$ shown in Fig.15, left. The set $\mathcal{R}_{1,1}$ in the plane of J-invariant is shown in Fig.15, right. The set $\mathcal{R}_{1,1}$ intersects the real line at the following theree approximate values of J - invariant:

$$J_1 \simeq -1690, \quad (x_1 \simeq 1.5538 + 0.2514i,\ x_2 \simeq 0.1650 - 0.4893i) \tag{6.9}$$

$$J_2 \simeq 586.3 \quad (x_1 \simeq 1.2551 + 0.1883i, \quad x_2 \simeq 0.6865 - 0.2986i) \tag{6.10}$$

$$J_3 \simeq 7791, \quad (x_1 \simeq 1.8037, \quad x_2 = -0.3797) \tag{6.11}$$

All three values J_i correspond to curves $\widehat{\mathcal{C}}$ possessing a real involution. However, only the value J_3 corresponds to the Boutroux-Krichever curve where the Abelian differential $v = \sqrt{Q}$ is invariant under this involution i.e. $v(\bar{x}) = \overline{v(x)}$.

6.3 Variation of $\arg \Delta^{\pm}_{-1,-1}$ on $\mathcal{Q}_0^{\mathbb{R}}([-3]^2)$

The goal of this section is to study the variation of the arguments of the expressions

$$\Delta^{+}_{-1,-1} := x_1^6 x_2^6 (x_1 - x_2)^2, \qquad \Delta^{-}_{-1,-1} := x_1^6 x_2^6 (x_1 - x_2)^{26} \tag{6.12}$$

over the space $\mathcal{Q}_0^{\mathbb{R}}([-3]^2)$. The origin of the expressions (6.12) lies in the formalism of Bergman tau-function [17, 14, 18, 19].

As well as the previos case, the arguments of $\Delta^{\pm}_{-1,-1}$ (6.12) do not change under simultaneous multiplication of all x_i with positive real constant. Therefore, $\arg \Delta^{\pm}_{-1,-1}$ is constant along any ray passing through the origin in the first octant of the (A, B)-plane. In particular, $\arg \Delta^{\pm}_{-1,-1}$ is constant on each of the rays $A = 0$, $B = 0$ and $A = B$.

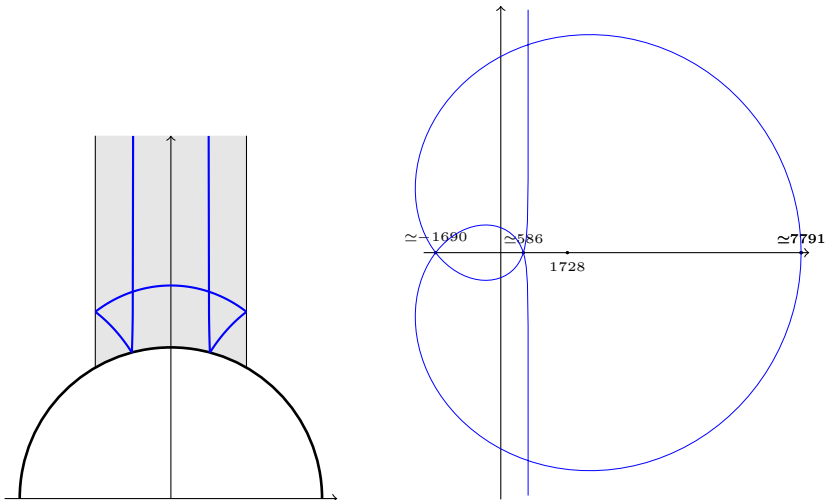

Figure 15: Left: the space $\mathcal{Q}_0^{\mathbb{R}}([-3]^2)$ is fibered over the shown curve $\mathcal{R}_{-1,-1}$ in the moduli space of elliptic curves with the fiber $\mathbb{R}_+$. Right: the set $\mathcal{R}_{-1,-1}$ in the plane of J-invariant. Three real curves correspond to values of J-invariant $J_1 \simeq -1690$, $J_2 \simeq 586$, $J_3 =\simeq 7791$.

Proposition 2 *Suppose that* $Q = \frac{(x-x_1)(x-x_2)}{x^3}\mathrm{d}x^2 \in \mathcal{Q}_0^{\mathbb{R}}([-3]^2)$. *Then*

1. *one root* x_i *is real if and only if the other is: moreover, they either coincide* ($x_1 = x_2 > 0$) *or one of them (say,* x_2*) is positive and the other* (x_1) *is negative. In this latter case, the horizontal trajectories connect* x_1 *to* 0 *along the negative axis, and* x_2 *to* $+\infty$ *along the positive axis.*

2. *if one root is in the upper half plane then the other is in the lower half plane;*

The proof of this proposition is technical; it is contained in the Appendix. In Fig. 16 we show how the branch points x_i and the horizontal trajectories evolve as periods (A, B) move from the point $(1, 0)$ to the point $(0, 1)$ along the straight line.

The previous proposition implies

Proposition 3 1. *As* $A \to 0$ *we have*

$$\arg x_{1,2} \to 0 \qquad \arg(x_2 - x_1) \to \pi/4 \tag{6.13}$$

2. *As* $A = B$ *we have*

$$\arg x_1 = 0 \qquad \arg x_2 = \pi \qquad \arg(x_2 - x_1) = 0 \tag{6.14}$$

3. *As* $B \to 0$ *we have*

$$\arg x_1 \to 2\pi \qquad \arg x_2 \to 0 \qquad \arg(x_2 - x_1) \to -\pi/4 \tag{6.15}$$

Proof. **[1]**. As the curve $\widehat{\mathcal{C}}$ degenerates, item 1 of Prop. 2 implies that $\arg_{1,2} \to 0$ and $x_{1,2} \to x_0 > 0$; in this limiting case the flat coordinate is $z(x) = \frac{\sqrt{x}}{2} + \frac{x_0}{2\sqrt{x}}$ and the critical trajectories $\operatorname{Re} z = 0$ are easily seen to consist of $\mathbb{R}_+ \cup \{|x| = x_0\}$.

By Prop. 2 the two roots remain in opposite half-planes; with our choice of A, B, it is clear that as A decreases, x_1 moves in the lower half-plane from $\mathbb{R}_-$ and x_2 in the upper half-plane from $\mathbb{R}_+$.

When $A \to 0$, we know that the curve degenerates and both roots converge to a point on $\mathbb{R}_+$; since they are confined in their respective half-planes, the statement about the increments of $\arg x_{1,2}$ follows immediately. As $A \to 0_+$, an analysis entirely similar to that of Lemma 4 (which we do not repeat), shows that $\lim_{A\to 0_+} \arg(x_2 - x_1) = \frac{\pi}{4}$. See also the numerically accurate Fig. 16.

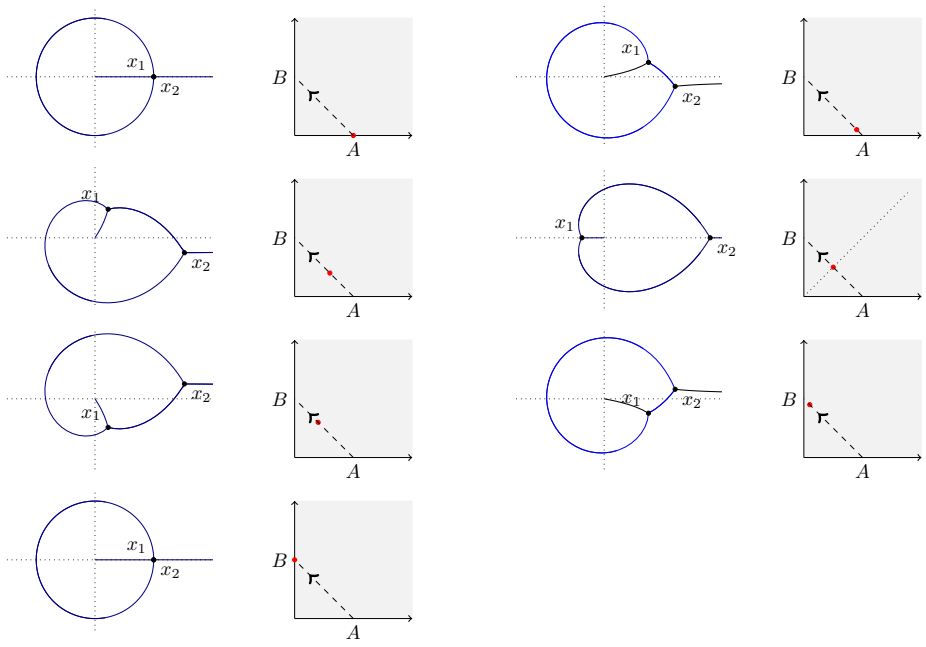

Figure 16: As the periods (A, B) move from the point $(1, 0)$ to the point $(0, 1)$ along the line $A + B = 1$, the root marked x_1 rotates counterclockwise around the origin. This move corresponds to monodromy around the point $Q = (dx)^2/x$ on the space $\widehat{Q}_0^{\mathbb{R}}([-3]^2)$.

[2]. From part 1 of Prop. 2 it follows that for $A = B$ we have $x_1 \in \mathbb{R}_-, x_2 \in \mathbb{R}_+$ and hence $\arg(x_2 - x_1) = 0$.
[3]. This case is obtained from case [1] by sending $v(x) \mapsto \overline{v(\overline{x})}$. ■

Finally we are in the position to formulate the second main analytical result:

Theorem 4 *The monodromies of* $\arg \Delta^{\pm}_{-1,-1}$ *(6.12) on the space* $\mathcal{Q}_0^{\mathbb{R}}([-3]^2)$ *along an elementary non-contractible loop equal* 13π *and* 25π*, respectively.*

Proof. It suffices to refer to Prop. 3 to compute the increments of $\arg \Delta^{\pm}_{-1,-1}$ from the diagonal $A = B$ to the boundary $A = 0$. Namely, for $A = B$ we have $\arg x_1 = -\pi$, $\arg x_2 = 0$, $\arg(x_2 - x_1) = 0$ and for $A = 0$ we have (in the limit) $\arg x_{1,2} = 0$, $\arg(x_2 - x_1) = \frac{\pi}{4}$. Hence the variations are $\frac{\pi}{2} + 6\pi = \frac{13}{2}\pi$ for $\Delta^{+}_{-1,-1}$ and $\frac{13}{2}\pi + 6\pi = \frac{25}{2}\pi$ for $\Delta^{-}_{-1,-1}$. To get the monodromy over the whole cell we must duplicate these increments. ■

Acknowledgements. D.K. thanks Peter Zograf for interesting discussions. The research of M. B. was supported in part by the Natural Sciences and Engineering Research Council of Canada grant RGPIN/261229–2011. The research of D.K. was supported in part by the Natural Sciences and Engineering Research Council of Canada grant RGPIN/3827-2015, Alexander von Humboldt Stiftung and GNFM Gruppo Nazionale di Fisica Matematica. Both authors were supported by the FQRNT grant "Matrices Aléatoires, Processus Stochastiques et Systèmes Intégrables" (2013–PR–166790). D.K. thanks the International School of Advanced Studies (SISSA) in Trieste and Max-Planck Institute for Gravitational Physics in Golm (Albert Einstein Institute) for their hospitality and support during the preparation of this paper.

A Proof of Proposition 2

[**1**] The Boutroux property (i.e. the reality of all periods) is invariant under the action of $\mathbb{R}_+$ that maps $x \mapsto \lambda x$, $x_j \to \lambda x_j$, $Q \mapsto \lambda Q$. Suppose that one of the roots x_j is real; depending on its sign, using the above

scaling, we can restrict ourselves by the case that this root equals ± 1. Let us therefore study the differentials

$$v_+ = \sqrt{\frac{(x-q)(x-1)}{z}}\frac{\mathrm{d}x}{x}, \quad \text{and} \quad v_- = \sqrt{\frac{(x-q)(x+1)}{x}}\frac{\mathrm{d}x}{x}\,. \tag{A.1}$$

Degenerate case. Suppose $q = 1$ for v_+ or $q = 1$ for v_-; then the resulting differential can be integrated explicitly

$$\int_1^x v_+ = 2\left(\sqrt{x} + \frac{1}{\sqrt{x}} - 2\right);, \qquad \int_{-1}^x v_- = 2\left(\sqrt{x} - \frac{1}{\sqrt{x}} - 2i\right)\,. \tag{A.2}$$

In the first case we see easily that the horizontal trajectories (where the real part of the integral vanishes) are $|x| = 1$ and $\mathbb{R}_+$. In the second case there is no trajectory connecting -1 to itself; this is seen by computing the integral along closed path connecting $x = -1$ to itself around the origin, and noticing that the result is actually imaginary.

Nondegenerate case. Let us show that the Boutroux condition makes q to be real and of the opposite sign (i.e. q is negative in the case of v_+ and positive in the case of v_-). We consider two cases separately.

Case +. Let us rewrite the periods by an integration by parts:

$$H(q) := \frac{1}{2}\int_{\gamma_1}\sqrt{\frac{(x-1)(x-q)}{x}}\frac{\mathrm{d}x}{x} \overset{b.p.}{=} \int_0^1 \frac{q+1-2x}{\sqrt{x(1-x)(q-x)}}\mathrm{d}x\,, \tag{A.3}$$

$$J(q) := \frac{1}{2}\int_{\gamma_q}\sqrt{\frac{(x-1)(x-q)}{x}}\frac{\mathrm{d}x}{x} \overset{\substack{b.p.\\ x\mapsto qx}}{=} \int_0^1 \frac{1+(1-2x)q}{\sqrt{x(1-x)(1-qx)}}\mathrm{d}x\,. \tag{A.4}$$

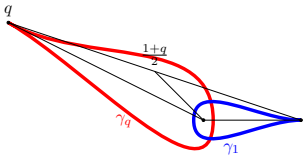

Figure 17: The contours of integration γ_1, γ_q.

Our goal is to show that the equations $\operatorname{Im} I(q) = 0 = \operatorname{Im} J(q)$ have only one solution $q^\star \in \mathbb{R}_-$.

We start by showing that the locus of the equation $\operatorname{Im} J = 0$ is the set $q \in (-\infty, 1]$. The function $J(q)$ is manifestly analytic in the domain $\mathcal{D} = q \in \mathbb{C} \setminus [1, \infty)$ and has a branch point at $q = 1$. A simple analysis of the integral (A.4) shows that

1. $\lim\limits_{q\to 0+i0} J(q) = \displaystyle\int_0^1 \frac{\mathrm{d}x}{\sqrt{x(1-x)}} = \pi.$
2. $\lim\limits_{q\to 1+i0} J(q) = 4;$
3. $J((-\infty, 1] + i0) = (-\infty, 4];$
4. for $q > 1$ the imaginary part of $J(q)$ (boundary value from upper half plane) is positive; this is the estimate in (A.7) below.

On the domain $\mathcal{D}$ we also have the Schwartz symmetry $\overline{J(\overline{q})} = J(q)$ and hence it suffices to study it in the upper half plane.

The locus $\operatorname{Im} J = 0$ is the union of possibly several smooth arcs, each of which must be extensible indefinitely until they reach either a singularity of $J(q)$ or a zero of $J'(q)$. We now show that $J'(q) \neq 0$ in $\mathcal{D}$; this is easily seen by explicit computations as follows

$$J'(q) = -\frac{1}{4}\int_{\gamma_q}\frac{\mathrm{d}x}{x}\sqrt{\frac{x-1}{x(x-q)}} \overset{b.p.}{=} -\frac{1}{4q}\int_{\gamma_q}\sqrt{\frac{q-x}{x(1-x)}}\mathrm{d}x \overset{z=qt}{=} -\frac{1}{2}\int_0^1\sqrt{\frac{1-t}{t(1-qt)}}\mathrm{d}t \tag{A.5}$$

The last integral is clearly always nonzero for all $q \in \mathcal{D}$.

Since there are no zeroes of $J'(q)$ in $\mathcal{D}$, any branch of $J^{-1}(\mathbb{R})$ that may be in $\mathbb{H}$ must extend to infinity along some direction or be a bounded curve starting and ending at $q=1$; this latter case is excluded because $\operatorname{Im} J$ is harmonic and bounded at $q=1$ and there are no singularities in $\mathcal{D}$.

Note that as $|q|\to\infty$ in the upper half plane, we have from (A.4) that $J(q)\sim i\sqrt{q}\ln(1-q)\sim\sqrt{-q}\ln(-q)$ and the real part (to leading order in $|q|$) is easily seen not to change sign for $0<\arg(q)<\pi$. Hence there are no branches of $J^{-1}(\mathbb{R})$ extending to infinity. To prove item 4 from the above list we observe that for $q>1$

$$\operatorname{Im} J(q)=\sqrt{q}\int_{\frac{1}{q}}^{1}\frac{q^{-1}+1-2x}{\sqrt{x(1-x)(x-q^{-1})}}= \tag{A.6}$$

$$=\sqrt{q}\int_{q^{-1}}^{\frac{q^{-1}+1}{2}}\frac{\overbrace{q^{-1}+1-2x}^{>0}}{\sqrt{x(1-x)(x-q^{-1})}}\mathrm{d}z+\sqrt{q}\int_{\frac{q^{-1}+1}{2}}^{1}\frac{\overbrace{q^{-1}+1-2x}^{<0}}{\sqrt{x(1-x)(x-q^{-1})}}\mathrm{d}x \tag{A.7}$$

To see that the result is positive we proceed to a simple estimate of the two integrals:

$$\int_{q^{-1}}^{\frac{q^{-1}+1}{2}}\frac{q^{-1}+1-2z}{\sqrt{x(1-x)(x-q^{-1})}}\mathrm{d}x>\int_{q^{-1}}^{\frac{q^{-1}+1}{2}}\frac{q^{-1}+1-2x}{\sqrt{\frac{q^{-1}+1}{2}(1-x)(x-q^{-1})}}\mathrm{d}x \tag{A.8}$$

and

$$\int_{\frac{q^{-1}+1}{2}}^{1}\frac{q^{-1}+1-2x}{\sqrt{x(1-x)(x-q^{-1})}}\mathrm{d}z>\int_{\frac{q^{-1}+1}{2}}^{1}\frac{q^{-1}+1-2x}{\sqrt{\frac{q^{-1}+1}{2}(1-x)(x-q^{-1})}}\mathrm{d}x\overset{x\mapsto 1+q^{-1}-x}{=} \tag{A.9}$$

$$=\int_{\frac{q^{-1}+1}{2}}^{q^{-1}}\frac{q^{-1}+1-2x}{\sqrt{\frac{q^{-1}+1}{2}(1-x)(x-q^{-1})}}\mathrm{d}x=-\int_{q^{-1}}^{\frac{q+1}{2}}\frac{q^{-1}+1-2x}{\sqrt{\frac{q^{-1}+1}{2}(1-x)(x-q^{-1})}}\mathrm{d}x \tag{A.10}$$

and therefore the sum (A.7) is strictly positive. In summary, the only branch $\operatorname{Im} J=0$ is $(-\infty,1]$. This ends the proof that $J(q)$ is real only on $(-\infty,1]$.

We now analyze the other integral $H(q)$ (A.3) on the real q–axis and show that it takes real values only for $q\in[1,\infty)\cup\{q^\star\}$ where $q^\star<0$. For $q\geq 1$ the integrand is a real valued function for $x\in(0,1)$.

Let us show that for $q\in[0,1)$ the imaginary part of $H(q)$ is strictly positive; indeed, for $0<x<q$ the integrand is real–valued and so the imaginary part is (this is analogous to the estimates A.8, A.9 with the replacement $q^{-1}\mapsto q$)

$$\operatorname{Im} H(q)=\int_{q}^{1}\frac{q+1-2x}{\sqrt{x(1-x)(x-q)}}=\int_{q}^{\frac{q+1}{2}}\frac{\overbrace{q+1-2x}^{>0}}{\sqrt{x(1-x)(x-q)}}\mathrm{d}z+\int_{\frac{q+1}{2}}^{1}\frac{\overbrace{q+1-2x}^{<0}}{\sqrt{x(1-x)(x-q)}}\mathrm{d}z \tag{A.11}$$

To see that the result is positive we proceed to a simple estimate of the two integrals:

$$\int_{q}^{\frac{q+1}{2}}\frac{q+1-2x}{\sqrt{x(1-x)(x-q)}}\mathrm{d}x>\int_{q}^{\frac{q+1}{2}}\frac{q+1-2x}{\sqrt{\frac{q+1}{2}(1-x)(x-q)}}\mathrm{d}x \tag{A.12}$$

$$\int_{\frac{q+1}{2}}^{1}\frac{q+1-2x}{\sqrt{x(1-x)(x-q)}}\mathrm{d}x>\int_{\frac{q+1}{2}}^{1}\frac{q+1-2x}{\sqrt{\frac{q+1}{2}(1-x)(x-q)}}\mathrm{d}x\overset{z\mapsto 1+q-x}{=}-\int_{q}^{\frac{q+1}{2}}\frac{q+1-2x}{\sqrt{\frac{q+1}{2}(1-x)(x-q)}}\mathrm{d}x \tag{A.13}$$

and therefore the sum (A.11) is strictly positive and so $\operatorname{Im} H(q)>0$ for $q\in[0,1)$.

Now let $q<0$; then

$$H(q)=i\int_{0}^{1}\frac{x+|q|+(x-1)}{\sqrt{x(1-x)(|q|+x)}}\mathrm{d}x \tag{A.14}$$

so that it is purely imaginary. The imaginary part is a monotone function:

$$\frac{\mathrm{d}}{\mathrm{d}q}\operatorname{Im} H(q) = -\frac{1}{2}\int_0^1 \frac{|q|+1}{\sqrt{x(1-x)(|q|+x)}(x+|q|)}\mathrm{d}x < 0. \tag{A.15}$$

It is easily seen that $\lim_{q\to-\infty} H(q) = i\int_0^1 \frac{\mathrm{d}x}{\sqrt{x(1-x)}} = i\pi$ while as $q \to 0_-$ the value of $H(q)$ diverges logarithmically to $-\infty$. Therefore it vanishes at a single point $q^\star < 0$.

Numerical analysis shows that

$$q^\star \simeq -0.21048557\ .$$

Case $-$. Two independent homological coordinates are given by the integrals

$$\widehat{H}(q) := \frac{1}{2}\int_{\gamma_{-1}} \sqrt{\frac{(x+1)(x-q)}{x}}\frac{\mathrm{d}x}{x} \overset{\text{b.p.}}{\underset{x\mapsto -x}{=}} \int_0^1 \frac{1-q+2x}{\sqrt{x(1-x)(q+x)}}\mathrm{d}x\ , \tag{A.16}$$

$$\widehat{J}(q) := \frac{1}{2}\int_{\gamma_q} \sqrt{\frac{(x+1)(x-q)}{x}}\frac{\mathrm{d}x}{x} \overset{\text{b.p.}}{\underset{x\mapsto qx}{=}} i\sqrt{q}\int_0^1 \frac{1-q^{-1}-2x}{\sqrt{x(x+q^{-1})(1-x)}}\mathrm{d}x\ . \tag{A.17}$$

- We first show that $\operatorname{Im} q > 0$ implies $\operatorname{Im}\widehat{H}(q) < 0$ and that $\widehat{H}(q) \in \mathbb{R}$ only for $q > 0$; this is easily seen by rewriting $\widehat{H}(q)$ as

$$\widehat{H}(q) = \int_0^1 \frac{1+3x}{\sqrt{x(1-x)(q+x)}}\mathrm{d}x + \int_0^1 \frac{-\sqrt{q+x}}{\sqrt{x(1-x)}}\mathrm{d}x\ . \tag{A.18}$$

  Suppose $\operatorname{Im} q > 0$; a simple inspection of phases confirms that the integrands in both integrals have negative imaginary part.

  Therefore the requirement $\operatorname{Im}\widehat{H} = 0$ implies $q \in \mathbb{R}$. Suppose that $q < 0$; then the integrals in (A.18) (the boundary value being taken from $\operatorname{Im} q > 0$) acquire an imaginary contribution from the integration over $x \in [0, \min(1,-q)]$ and both contributions have negative imaginary part. We conclude that $q \in \mathbb{R}_+$.

- Having now restricted q to $\mathbb{R}_+$ we must see when the integral $\widehat{J}(q)$ is real for $q \in \mathbb{R}_+$. For $q > 0$ it is clear that $\widehat{J}(q) \in i\mathbb{R}$ and hence we are looking at the zeroes of $\widehat{J}(q)$ on $q \in \mathbb{R}_+$. An elementary analysis shows that $\operatorname{Im}\widehat{J}(q)$ is an increasing function of $q \in \mathbb{R}_+$ which changes sign only once. Hence $\widehat{J}(q)$ is real only at one point $\tilde{q}r$, which must then be obtained by the dilation action from the previous case, so that $\tilde{q} = -\frac{1}{q^\star} > 0$.

We finally show that the negative root is connected to zero by a horizontal trajectory; since the whole set of trajectories trajectories must be invariant under $z \mapsto \overline{z}$, if a trajectory issuing from either root runs along the real axis, it must be either a segment to 0 or a ray to ∞. An elementary local analysis shows that the asymptotic directions of every critical trajectory falling towards 0 go along $\mathbb{R}_-$ and those approaching ∞ go along $\arg(z) = 0$. Thus necessarily the negative root is connected to 0 and the positive root is connected to $+\infty$.

[2] In item **[1]** we proved that either both roots have nonzero imaginary part or they are both real; therefore, if they are not real, they either are in the same upper/lower half plane or in the opposite ones. Let us show it is the latter case. To see that it is sufficient to compute the differential with respect to the periods at the point where both roots are real.

So let $v = \sqrt{(x-x_1)(x-x_2)/x}\,\mathrm{d}x$ with $x_1 = 1, x_2 = q^\star$; we want to find what happens under an infinitesimal Boutroux deformation of x_0, x_1 (a deformation that preserves the Boutroux condition). A trivial computation yields (dot denotes a derivative with respect to some real deformation parameter t at $t = 0$)

$$\dot{v} = \frac{-x_1\dot{x}_2 - x_2\dot{x}_1 + (\dot{x}_1+\dot{x}_2)x}{2x\sqrt{x(x-x_1)(x-x_2)}}\mathrm{d}x \tag{A.19}$$

where $\dot{x}_1, \dot{x}_2$ are constrained by the requirement that all periods are real: for example if the deformation is $\dot{A} = 1, \dot{B} = 0$ then we would require that the periods of $\dot{v}$ are the given ones, which uniquely determines the coefficients $\dot{x}_1, \dot{x}_2$. Since we are computing the deformation at $x_1 = 1, x_2 = q^\star \in \mathbb{R}_-$ we can write,

$$\dot{v} = \frac{-\dot{x}_2 - q^\star \dot{x}_1 + (\dot{x}_1 + \dot{x}_2)x}{2x\sqrt{x(x-1)(x-q^\star)}}\mathrm{d}x \tag{A.20}$$

Consider now the period from $x = 1$ to $x = \infty$;

$$-(\dot{x}_2 + q^\star \dot{x}_1)C_0 + (\dot{x}_1 + \dot{x}_2)C_1 = \alpha \in \mathbb{R}\,; \tag{A.21}$$

$$C_j = \int_1^\infty \frac{x^j \mathrm{d}x}{\sqrt{x(x-1)(x-q^\star)}}. \tag{A.22}$$

It is evident that C_j's are real and of the same sign depending on the chosen determination of the square root (say, positive). Moreover it is also evident that $|C_1| > |C_0|$ because the integration is on $[1, \infty)$; taking the imaginary part of (A.22) yields

$$-C_1 \operatorname{Im}(q^\star \dot{x}_1 + \dot{x}_2) + C_0 \operatorname{Im}(\dot{x}_1 + \dot{x}_2) = 0 \in \mathbb{R} \quad \Rightarrow \quad \operatorname{Im}\dot{x}_2 = \frac{C_0 - q^\star C_1}{C_0 - C_1}\operatorname{Im}\dot{x}_1. \tag{A.23}$$

The coefficient $\frac{C_0 - q^\star C_1}{C_0 - C_1}$ is negative because C_0, C_1 are of the same sign, $q^\star \simeq -0.2$ is negative and $|C_1| > |C_0|$. Thus the initial directions of the motion of the two roots point to the opposite half-planes. By a simple continuity argument, the points $x_{1,2}$ cannot cross the real axis without falling onto the case covered by the previous analysis. Hence they remain confined within opposite half-planes. ■

References

[1] E.Arbarello, M.Cornalba, *Combinatorial and algebro-geometric cohomology classes on the moduli spaces of curves*, J.Algebraic Geometry **5** No.4, 705-749 (1996)

[2] M.Bertola, *Boutroux curves with external field: equilibrium measures without a variational problem.* Anal. Math. Phys. **1** no. 2-3, 167211 (2011)

[3] , M. Bertola, D. Korotkin, *Tau-functions on spaces of meromorphic differentials and Jenkins-Strebel combinatorial model of $M_{g,n}$* , to appear (2017).

[4] Boutroux, P., *Recherches sur les transcendantes de M. Painlevé et l'étude asymptotique des équations différentielles du second ordre*, Ann. Sci. École Norm. Sup. (3) **30**, 255375 (1913) and **31**, 99159 (1914)

[5] B.Dubrovin, *Geometry of 2D topological field theories*, in: "Integrable systems and quantum groups" Lecture Notes in Math., v.1620, Springer, Berlin, 120348 (1996)

[6] Fokas, A., Its, A., Kapaev, A., Novokshenov, V., *Painlevé transcendent. The Riemann-Hilbert approach.* Mathematical Surveys and Monographs, **128**, AMS, Providence, RI, 2006, 553 pp.

[7] J.Harer, *The Cohomology of the Moduli Space of Curves* , Theory of moduli (Montecatini Terme, 1985), 138221, Lecture Notes in Math., 1337, Springer, Berlin (1988)

[8] J.Harer, *The virtual cohomological dimension of the mapping class group of an orientable surface*, Invent.Math. **84** no. 1, 157176 (1986)

[9] K. Igusa, *Graph cohomology and Kontsevich cycles*, Topology, bf 43 1469-1510 (2004)

[10] K. Igusa, *Combinatorial Miller-Morita-Mumford classes and Witten cycles*, Algebraic and Geometric Topology, **4**, 473-520 (2004)

[11] J.Jenkins, *On the existence of certain general extremal metrics*, Ann. of Math. (2) **66** 440453 (1957)

[12] M.Kontsevich, *Intersection Theory on the Moduli Space of Curves and the Matrix Airy Function*, Commun. Math. Phys. **147** 1-23 (1992)

[13] M. Kontsevich, *Feynman diagrams and low-dimensional topology*, First European Congress of Mathematics, Vol. II (Paris, 1992), Birkhaüser, Basel, p. 97-121 (1994)

[14] A. Kokotov, D. Korotkin, *Tau-functions on spaces of Abelian differentials and higher genus generalization of Ray-Singer formula*, J. Diff. Geom. **82** (2009), 35-100

[15] A.Kokotov, D.Korotkin, *"Tau-functions on spaces of Abelian and quadratic differentials and determinants of Laplacians in Strebel metrics of finite volume"* math.SP/0405042, preprint No. 46 of Max-Planck Institute for Mathematics in Science, Leipzig (2004)

[16] I.M. Krichever, *The τ-function of the universal Whitham hierarchy, matrix models and topological field theories*, Comm. Pure Appl. Math. **47** (4) 437475 (1994)

[17] D.Korotkin, *Solution of matrix Riemann-Hilbert problems with quasi-permutation monodromy matrices*, Math. Ann. **329**, 335364 (2004)

[18] D.Korotkin, P.Zograf, *Tau function and moduli of differentials*, Math. Res. Lett. **18** No.3 (2011)

[19] D.Korotkin, P.Zograf, *Tau-function and Prym class*, Algebraic and geometric aspects of integrable systems and random matrices, 241261, Contemp. Math., 593, AMS, Providence, RI, 2013.

[20] A.Kokotov, D.Korotkin, P.Zograf, *"Isomonodromic tau function on the space of admissible covers"*, Advances in Mathematics, 227:1 586-600 (2011)

[21] A.Kokotov, D.Korotkin, Isomonodromic tau function of Hurwitz Frobenius manifolds and its applications, IMRN, **2006** 1-34 (2006)

[22] G.Mondello, *Riemann surfaces, ribbon graphs and combinatorial classes*, Handbook of Teichmller theory. Vol. II, 151215, IRMA Lect. Math. Theor. Phys., 13, Eur. Math. Soc., Zrich, 2009

[23] G. Mondello, *Combinatorial classes on $\overline{\mathcal{M}}_{g,n}$ are tautological*, Int. Math. Res. Not. **2004**, no. 44, 23292390 (2004)

[24] R.Penner, *The simplicial compactification of Riemanns moduli space*, Topology and Teichmuller spaces (Katinkulta, 1995), World Sci. Publishing, River Edge, NJ, pp. 237252 (1996)

[25] K.Strebel, *Quadratic differentials*, Springer, Berlin (1984)

[26] E.Witten, *Two-dimensional quantum gravity and intersection theory on moduli space*, Surveys in Differential Geometry, **1** 243-310 (1991)

[27] Lee, S.-Y.; Teodorescu, R.; Wiegmann, P. Shocks and finite-time singularities in Hele-Shaw flow. Phys. D 238 (2009), no. 14, 11131128.

[28] D.Zvonkine, *Strebel differentials on stable curves and Kontsevichs proof of Wittens conjecture*, 2004